UNIVERSITY OF MANITOBA

Analysis of Two-Phase Flow Patterns of Condensing Steam Inside a Horizontal Tube

by

Ali M. Fathi

A Thesis

Submitted to the Faculty of Graduate Studies
in Partial Fulfillment of the Requirements for the
Master of Science Degree in Mechanical Engineering

Winnipeg, Manitoba

1980

Analysis of Two-Phase Flow Patterns of Condensing Steam Inside a Horizontal Tube.

by

Ali M. Fathi

A thesis submitted to the Faculty of Graduate Studies of the University of Manitoba in partial fulfillment of the requirements of the degree of

Master of Science

TABLE OF CONTENTS

ABSTRACT

A comprehensive review of the literature on two-phase flow patterns of condensing fluids inside horizontal tubes revealed limited information. Most of the published data correspond to two fluids, Freon-12 and Freon-113, condensing in tubes ranging in inside diameters between 0.1875 in. and 0.625 in. In the meantime, there are no established criteria for the prediction of flow patterns during condensation. The main objectives of the present investigation are to generate new data using steam as the test fluid and to study the applicability of different correlations (empirical and theoretical) for the prediction of flow patterns during condensation. Steam was selected as the test fluid because it is widely different in physical and transport properties from other fluids tested earlier.

An experimental set-up was designed and constructed to achieve the objectives of the present study. The test condenser has 0.527 in. I.D. for the inner tube. Data were obtained covering a wide range of steam mass flow rates, inlet superheats, pressures, and cooling rates. The major flow patterns which were observed were: spray, annular, wavy, slug, plug, and stratified. In addition, two transitional flow patterns were reported; these are the spray-annular, and annular-wavy. It was not possible to calculate

flow-map parameters for the slug, plug, and stratified flow patterns since the heat balance resulted in sub-cooled conditions for these observations. As a result, these flow pattern observations were not correlated.

The present data, as well as others reported in the literature, were compared with the most widely known empirical flow pattern correlations. It was concluded that Baker's [5]* map failed in predicting the present data, however, a map developed for condensation, by Soliman [19] using Baker's coordinates agreed fairly well with the present data. Another set of coordinates suggested in [19], namely the void fraction and the velocity of the liquid phase V_ℓ, was tested with the present data and found to be a possible basis for a generalized correlation for condensation. On the other hand, the superficial liquid velocity versus superficial gas velocity coordinate system used by Mandhane et al. [12] failed in absorbing influences of fluid properties.

Comparisons were also done with the few theoretical correlations available in the literature. Traviss and Rohsenow [18] developed equations for the line separating the annular and the wavy flow patterns. The present data agreed very well with their prediction. Also, a reasonable agreement was found when this correlation was tested against

*Numbers in brackets denote references at end of thesis.

data of other fluids. Only the annular-wavy and annular-slug boundaries of Taitel and Dukler [14] theoretical map were tested. These transition lines were selected because they were the ones relevant to the present study. The slug flow data points reported in other studies did not correlate well with their predictions. However, the agreement with annular and wavy data points from present and other studies were considered to be satisfactory. The boundaries developed by Breber et al. [22] using Taitel and Dukler [14] coordinates were found to predict well the data of the present investigation.

The simple empirical criterion developed by Soliman [19] for the spray to annular transition was tested using the present data. Agreement was fair.

ACKNOWLEDGEMENTS

The author wishes to thank Dr. H.M. Soliman for his continuing interest and guidance without which this thesis would have been impossible. Special thanks are due to Dr. G.E. Sims for his helpful suggestions and encouragement. Thanks are also due to Dr. D.W. Trim.

The author would like to thank Mr. O. Tonn the Chief Technician in the Department of Mechanical Engineering of the University of Manitoba. Thanks are also due to all the technicians in the above-mentioned Department particularly Mr. M. Kapitoler.

Special thanks are due to all my colleagues especially Mr. A. Lau who assisted in the calibration of some of the equipment. Thanks are also due to Mrs. P. Giardino for typing the manuscript.

The author acknowledges the financial support received from the Department of Mechanical Engineering in the University of Manitoba in the form of teaching assistantship. The financial support provided by the University of Manitoba in the form of Graduate Fellowship is also acknowledged. The author also acknowledges the financial support from the Natural Sciences and Engineering Research Council of Canada under research Grant No. A0409.

The author is especially grateful to his wife. Her continuing encouragement, patience, and sacrifices made this work possible.

Finally the author would like to dedicate this thesis to his home country "Egypt".

LIST OF FIGURES

LIST OF TABLES

NOMENCLATURE

English Symbols:

A	Tube inside flow area (ft^2)
A_v	Vapor flow area (ft^2)
C_g	Gas percentage, defined by equation (2.4)
D	Tube inside diameter (ft)
$(dP/dx)_\ell$	Pressure drop for the liquid phase
$(dP/dx)_v$	Pressure drop for the vapor phase
F	Taitel and Dukler [14] parameter, defined by equation (4.4)
g	Gravitational acceleration (ft/sec^2)
g_c	Newton's proportionality constant = 32.174 lb_m ft/lbf sec
G	Total mass velocity ($lb_m/hr\ ft^2$)
G_ℓ	Liquid mass velocity = $(1 - x)G$ ($lb_m/hr\ ft^2$)
G_v	Vapor (gas) mass velocity = xG ($lb_m/hr\ ft^2$)
N_{CA}	Capillary number, defined by equation (4.11)
N_{FR}	Froude number, defined by equation (2.6)
N_{FR_ℓ}	Froude number of the liquid [18]
N_{GA}	Galileo number of the liquid, defined by equation [4.3e]
N_{RE}	Reynolds number, defined by equation (4.10)
N_{RE_ℓ}	Reynolds number of the liquid, defined by equation (4.3d)
N_{WE}	Weber number, defined by equation (4.7)

Q_ℓ	Liquid volumetric flow rate (ft^3/sec)
Q_v	Vapor volumetric flow rate (ft^3/sec)
R	Vapor volumetric ratio, defined by equation (2.5)
$V_{\ell s}$	Superficial liquid velocity = G_ℓ/ρ_ℓ (ft/sec)
V_{vs}	Superficial vapor velocity = G_v/ρ_v (ft/sec)
V_ℓ	Average liquid velocity, defined by equation (4.1)
V_m	Mixture velocity, defined by equation (2.3)
x	Dryness fraction
X or X_{tt}	Lockhart Martinelli [2] parameter

Greek Symbols

α	Void fraction = A_v/A
λ	Baker's [5] parameter, defined by equation (2.1)
μ_ℓ	Liquid dynamic viscosity (centipoise) or $lb_m/ft\ sec$)
μ_v	Vapor dynamic viscosity ($lb_m/ft\ sec$)
ν_ℓ	Liquid kinematic viscosity (ft^2/sec)
ρ_{av}	Average density of the mixture defined by equation (4.8)
ρ_ℓ	Saturated liquid density (lb_m/ft^3)
ρ	Saturated vapor density (lb_m/ft^3)
σ	Liquid surface tension (dyne/cm) or (lb_f/ft)
ψ	Baker's [5] parameter, defined by equation (2.2)

CHAPTER I

INTRODUCTION AND DEFINITIONS

1.1 Introduction

The simultaneous flow of two phases inside or outside a duct is known in the literature as two-phase flow. The two phases may belong to the same substance, (usually referred to as two-phase, one-component), or to two different substances with different chemical compositions, (two-phase, two-component). Pumping of mixtures of oil and natural gas, flow of gases and liquids in chemical contactors, hydraulic conveying of wheat, pulverized coal and ores, and material handling in food processing are some applications of two-phase, two-component flows. Examples of engineering equipment in which two-phase, one-component flows occcur are the boiler tubes in steam power plants, heat transfer equipment such as evaporators and condensers of refrigeration systems, and the cooling systems of nuclear reactors.

Experimental observations revealed that one or two-component two-phase flows assume different possible flow configurations. These configurations are called flow patterns or flow regimes and will be defined later in this chapter. Each flow pattern has its own heat, mass and momentum transfer characteristics, and consequently each

should have its own pressure drop and heat transfer correlations. Hence, from a designer point of view, the understanding of the hydrodynamic behavior of two-phase flow is important as well as necessary for achieving improved design for equipment in which such flows occur. In addition, being able to predict the flow patterns associated with different two-phase flow conditions is as crucial as knowing whether the flow is laminar or turbulent in single-phase flow.

Several research efforts dealing with two-phase, two-component (gas-liquid), adiabatic flow were reported in the literature. These investigations resulted in some information about the possible flow patterns, phase distributions, and pressure drop associated with the flow. Several correlations (empirical and analytical) for the prediction of flow patterns expected under certain conditions, were also suggested. Most of these correlations are limited in use to specific flow conditions, while few are claimed to be applicable to a wide range of flow conditions. An example of these correlations is presented later in this chapter.

Recently, a great deal of interest has been directed towards the study of two-phase, one-component, diabatic flows. This type of flow includes both boiling and condensation cases. When heat transfer is associated with the

flow it causes phase changes and changes in phase distribution along the duct. Consequently, the flow pattern never becomes fully developed and it changes continuously in the direction of the flow. In spite of the added complexity, few studies were successful in providing information on the flow patterns, pressure drop, and heat transfer characteristics.

A comprehensive review of published literature on the flow patterns of condensing fluids inside horizontal tubes revealed that the available information is quite limited. Most of the data correspond to two fluids (Freon-12 and Freon-113), and a limited range of tube diameters. In addition, there is no established correlation (empirical or analytical) for the prediction of flow patterns during condensation. More research efforts are required in this area and the present investigation was carried out as a first step. The objectives of this investigation are:

1. To design and construct an experimental facility for the study of flow patterns of condensing fluids inside horizontal tubes.
2. To generate flow pattern data for steam condensing inside a 0.527 in. I.D. horizontal tube.
3. To compare the obtained data with empirical and analytical flow pattern correlations available in the literature. Also, using other data reported earlier for fluids other

than steam, the influence of fluid properties on the transition criteria between different flow patterns will be investigated.

1.2 Definitions

Some of the terms mentioned above will be used extensively in this thesis, and hence, a proper definition is necessary. The term "flow pattern" is used to describe the different configurations which appear during two-phase flow. The type of flow pattern existing at a certain location within a tube depends on many factors, such as mass flow rates of the two phases, physical and transport properties, and tube diameter and orientation. During adiabatic gas-liquid flows the flow pattern does not change between the inlet and outlet of the duct, while for diabatic flows the pattern changes continuously in the direction of the flow due to heat transfer.

Figure 1.1 shows schematic diagrams of the different flow patterns associated with gas-liquid flows inside horizontal tubes [4]. The different descriptions used in identifying these patterns were:

Bubble flow: flow in which bubbles of gas move along the upper part of the pipe.

Stratified flow: flow in which the liquid flows along the bottom of the pipe and the gas flows above it over a smooth liquid-gas interface.

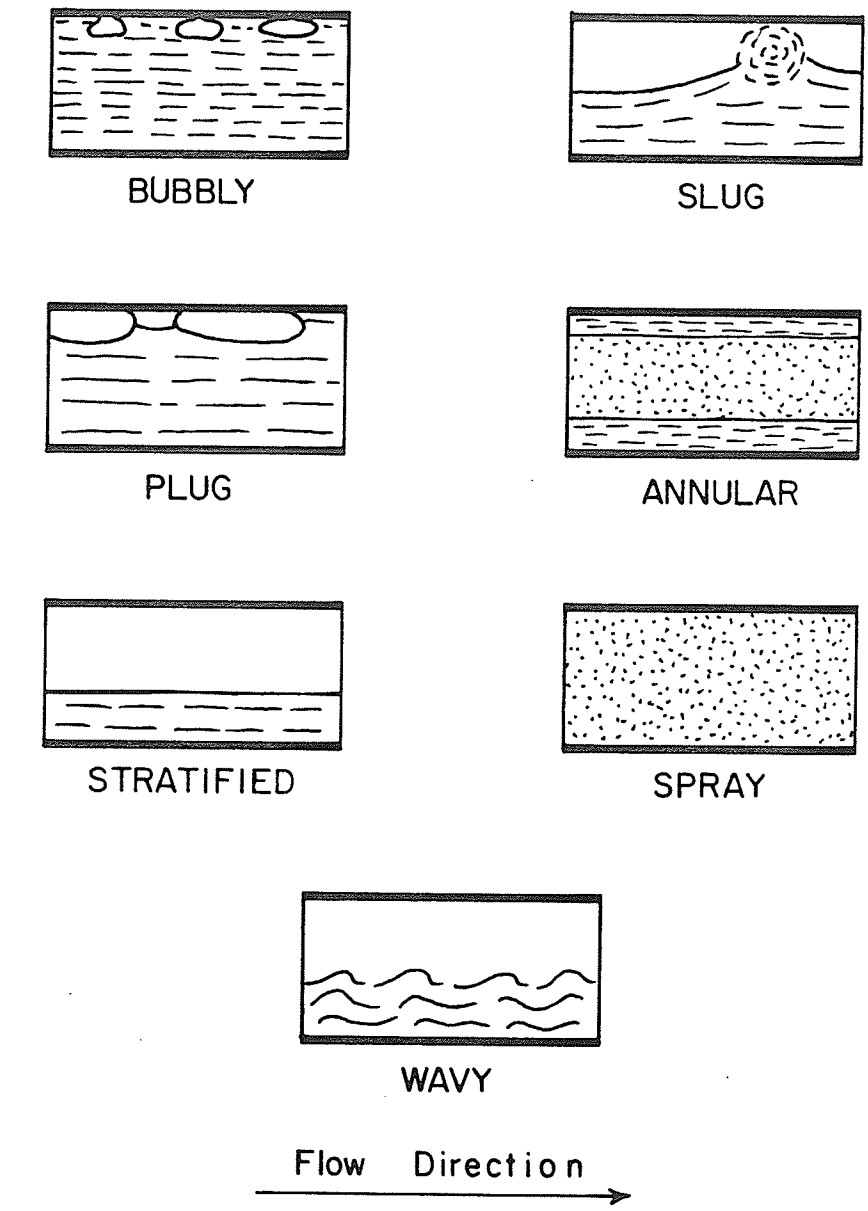

Fig. 1.1 Schematic diagrams of flow patterns of air-water inside a 1 in. I.D. horizontal tube [4].

Wavy flow: flow which is similar to stratified flow except that the gas moves at a higher velocity and the interface is disturbed by waves traveling in the direction of flow.

Slug flow: flow in which a wave is picked up periodically by the more rapidly moving gas to form a frothy slug which passes through the pipe at a much greater velocity than the average liquid velocity.

Annular flow: flow in which the liquid flows in a film around the inside wall of the pipe and the gas flows at a high velocity as a central core.

Spray flow: flow in which most or nearly all of the liquid is entrained as spray by the gas.

Usually, each investigator reported descriptions for the different flow patterns observed during his experiment. There is a fairly common agreement among investigators on these descriptions, and hence the above ones are considered representative of the literature. To give an idea about the types of flow expected during condensation, Fig. 1.2 shows the development of the flow patterns along the axis of a horizontal tube.

An example of the correlations developed in the literature [4] for the prediction of flow patterns expected at certain conditions is shown in Fig. 1.3. In preparing this correlation [4] the different flow pattern observations were

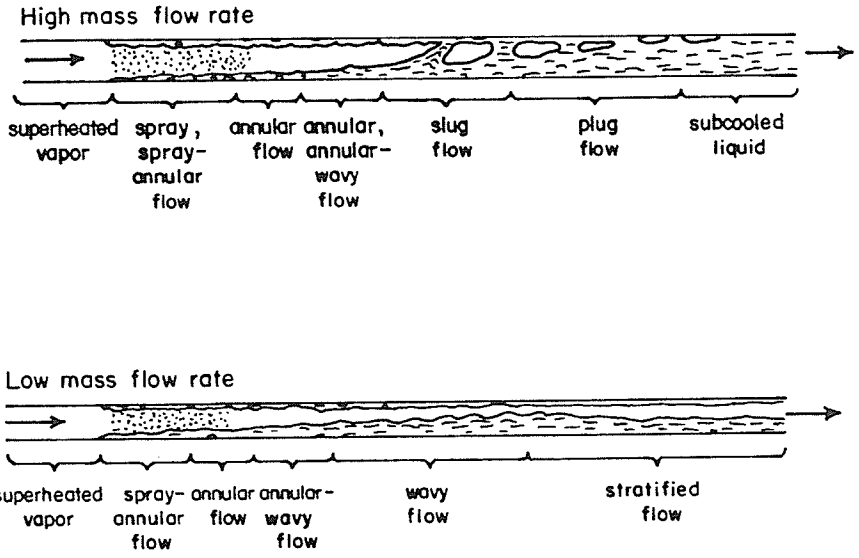

Fig. 1.2. Flow pattern development during condensation inside horizontal tubes.

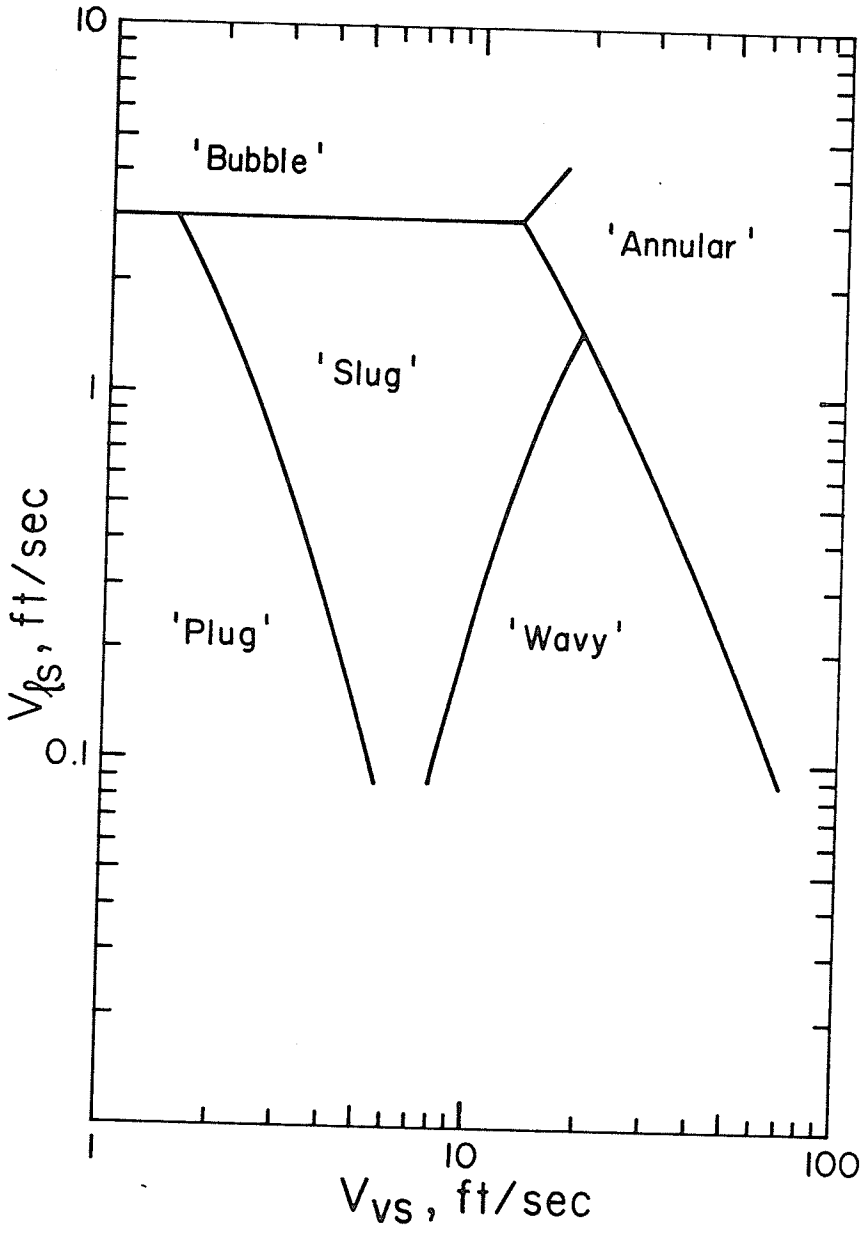

Fig. 1.3 Flow map for air-water flow inside a 1 in. I.D. horizontal tube [4].

plotted on a map using a certain coordinate system. Data of each flow pattern occupied an area on this map. Transition lines between different areas were then drawn arbitrarily, with the understanding that each of these lines represent in fact a transition zone with a finite width. Several of these correlations were reported, using different coordinate systems. This is an area where there is no agreement in the literature and it is for this reason that this research project was undertaken.

CHAPTER 2

LITERATURE REVIEW

Investigations dealing with the two-phase flow patterns of condensing fluids inside horizontal tubes are quite limited. In order to gain a better understanding of the problem, the scope of literature search was widened to include some of the references dealing with adiabatic two-phase, two-component flow patterns. This proved beneficial since there are many common features between these two types of flow, as well as similarities in the experimental techniques and methods of data presentation. The present review is divided into two parts; the first relates to adiabatic cases, while the second relates to diabatic (mainly condensation) studies.

2.1 Adiabatic Flow Studies

This part of the literature review is not intended to be a comprehensive one; only a selected portion of reported investigations is included. One of the earliest two-phase flow studies was done by Martinelli *et al.* [1]. Their objective was to investigate the effect of pipe diameter, rate of liquid and gas mass flow, liquid viscosity, liquid and gas density, and gas viscosity on the pressure drop during two-phase flow. Data were collected from two test sections; a 1 in. I.D. glass tube and a 0.5 in. I.D. galvanized iron pipe. The gas phase was air, while water,

kerosene, benzene, diesel fuel and S.A.E. 40 oil were used as test liquids. Flow combinations varied from all-air to all-liquid conditions. The existence of different flow patterns at various flow conditions was noticed. These different flow patterns were documented by photographs and sketches, but no descriptions were reported. Also no attempt was made to relate the pressure drop measurements to the types of flow pattern observed. Later, Lockhart and Martinelli [2] presented two-phase pressure drop data for the simultaneous flow of air and liquids including benzene, kerosene, water and oil in pipes varying in diameter from 0.586 in. to 1.017 in. This study resulted in one of the most widely used correlations for pressure drop in two-phase flow. This correlation, while still independent of the type of flow pattern existing, classifies the flow into four categories depending on whether each phase is flowing laminarly or turbulently.

A study of the different flow patterns associated with gas-liquid flow was reported by Bergelin and Gazley [3]. They experimentally investigated the flow of air and water in a 1 in. I.D. horizontal glass tube. Observed flow patterns were divided into three types; unsteady type (including bubble, wavy, and slug flows), steady type (annular flow), and a steady type with respect to time but not with respect to distance (stratified flow). The generated flow pattern

data were correlated in a map using the air and water mass flow rates as coordinates. Alves [4] conducted an experimental investigation of the isothermal flow of water-air and oil-air mixtures in a 1 in. co-current pipe line contactor. Flow pattern, pressure drop and liquid holdup data were obtained at various constant liquid flow rates and a range of air rates at or near room temperature. Different flow patterns, including bubble, plug, stratified, wavy, slug, annular, and spray, resulted in this study and descriptions and photographs were reported. Flow pattern data were correlated by map using superficial gas and liquid velocities as coordinates, (shown earlier in Fig. 1.3).

All the flow pattern maps mentioned so far are limited in use to conditions of tube diameters and gas-liquid combinations similar to those from which each map was constructed. Baker [5] noted that and made the first attempt at constructing a generalized map for the adiabatic two-phase flow patterns inside horizontal tubes. He used data of other investigators (e.g., [4]) covering a wide range of tube diameters and gas-liquid combinations and prepared a map using coordinates which are functions of the superficial mass velocities G_v and G_ℓ. To account for the properties of the flowing mixture, Baker [5] used the following correction factors introduced earlier by Holmes [6] for correlating the flooding in wetted wall distillation columns:

$$\lambda = [(\rho_v/0.075)\ (\rho_\ell/62.3)]^{1/2} \tag{2.1}$$

and

$$\psi = (73/\sigma)\ [\mu_\ell\ \ (62.3/\rho_\ell)^2]^{1/3} \tag{2.2}$$

This map, because of its wide base of experimental data, is commonly known in the literature and will be referred to in later chapters.

The influence of tube diameter and properties of the flowing mixture on the transition lines of flow pattern maps was explored in some additional research efforts. Hoogendoorn [7] studied experimentally the flow patterns during gas-liquid flows in smooth pipes of 0.945, 1.97, 3.58, and 5.51 in. inside diameters. Water, spindle oil, and gas oil were used as liquids, while air at pressures ranging between 1 and 3 atm was used as the gas phase. Flow pattern data were presented in a map using, as coordinates, the mixture velocity V_m and gas percentage C_g defined by

$$V_m = \frac{Q_v + Q_\ell}{\frac{\pi}{4}(D^2)}\ , \tag{2.3}$$

and

$$C_g = \frac{Q_v}{Q_v + Q_\ell} \times 100\ . \tag{2.4}$$

A shift in the transition lines accompanied any change in pipe diameter or test liquid. Hoogendoorn [7] found these shifts to be small and pointed out the fact that the

transition lines on any map should be viewed as representing a zone rather than a sharp line. Because air was the only gas tested in [7], Hoogendoorn postulated that larger deviations in the transition lines might result from different gas densities. To explore this possibility, Hoogendoorn and Buitelaar [8] experimentally investigated the flow of superheated Freon-11 vapor and water, as well as the flow of flashing Freon-11, in a horizontal 5.91 in. I.D. pipe. The map developed in [7] was found to correlate the obtained data adequately, thus ruling out the possibility of a strong influence of gas density on the transition lines.

More flow pattern data resulted from the investigation by Govier and Omer [9] corresponding to air-water flow in 1.026 in. I.D. horizontal pipe. The average system pressure was held constant at 36 psi maintaining a constant air density of 0.18 $lb_m/ft.^3$ Flow pattern, holdup and pressure drop data were obtained at air-water volume ratio from 0.1 to 200 for 10 superficial water velocities from 0.01 to 5.03 ft/sec. The flow patterns observed at constant superficial water velocity with increasing air-water ratio were: bubble, plug, stratified, wave, slug, and film (annular). Visual observations were correlated in a map having G_ℓ and G_V as coordinates. Later, Govier and Aziz [10] modified the transition lines of this map and presented a revised version using V_{VS} and $V_{\ell S}$ as coordinates. In preparing this

revised map, Govier and Aziz took into consideration the holdup data as well as visual observation in replotting the transition lines. This was done by directly correlating the major flow pattern transitions with the loci of the maximum and minimum points in the holdup curves. Govier and Aziz considered this revised map to be accurate for air-water flow in a 1 in. I.D. pipe and, based on the observations of Hoogendoorn [7], they recommended it for other practical applications. Scott [11] used the data reported in [7] and [9] to modify Baker's [5] map. The modification amounted to redrawing some of the transition lines as areas of finite width in order to account for variations in tube diameter and fluid properties.

One of the most recent flow pattern maps for adiabatic, two-phase flow in horizontal tubes is that developed by Mandhane et al. [12]. This map is based on 5,935 flow pattern observations collected from different investigations and covering a wide range of tube diameters, gas and liquid densities, gas and liquid viscosities, surface tension, and gas and liquid flow rates. Superficial liquid velocity and superficial gas velocity were used as coordinates. For simplicity, the transition lines were generated first from air-water data and physical property corrections were then made to extend the applicability of the map to other gas-liquid combinations. These corrections were applied to

the transition lines, rather than to the axes of the map as was done by Baker [5]. Mandhane et al. [12] tested their map as well as the other maps reported in [5], [7], and [10] on the accuracy of predicting actual flow pattern observations. They concluded that their map is in substantially better agreement with the air-water data than any of the other maps tested, and it is in slightly better agreement with the overall data. Reference to this map will be made in a later chapter.

A general conclusion that can be drawn from the above references is that there is no standard method developed yet in the literature for the presentation of flow pattern data. Different coordinate systems were used by different investigators in generating their maps. The lack of standard coordinates is a result of the lack of knowledge with respect to the most relevant parameters governing the stability of each flow pattern and the criteria of transition from one pattern to another. Due to the complexity of this problem, only a few simplified attempts were made to resolve it. Two analytical studies concerned with the transition criteria between different flow patterns are presented here: one dealing with the flow in vertical ducts [13] and the other with the flow in horizontal and near-horizontal tubes [14].

Quandt's [13] theoretical attempt was based on some assumptions which limited the forces acting on a fluid element

to the following:

- axial pressure gradient forces,
- gravitational attraction forces,
- interfacial surface tension forces.

After deriving mathematical formulae for these forces, Quandt suggested that the type of flow pattern existing at certain conditions depends on which of these three forces is dominant. He classified the bubble, annular, and spray flow patterns as pressure gradient controlled; the slug, wavy, and stratified as gravity controlled; and the capillary bubbles (in very small diameter tubes) as surface tension controlled. Transition from one group to another was assumed to take place when the two corresponding dominant forces are equal. Based on that, Quandt derived equations for two transition lines which were shown to agree fairly well with the empirical map by Baker [5] for certain flow conditions. Although this analysis is not complete, however, it resulted in some dimensionless groups, such as the Froude number and the Weber number, which were used later by other investigators in correlating their data.

A more refined analysis was reported recently by Taitel and Dukler [14] following an approach based on physically realistic mechanisms. The flow patterns considered were intermittent (slug and plug), stratified, wavy, bubble, and annular. The variables considered were the gas and liquid

mass flow rates, properties of the fluids, pipe size, and angle of inclination to the horizontal. Due to the fact that in many cases stratified flow exists at the pipe inlet, the analysis started by visualizing this particular flow pattern with the presence of a wave on the surface over which gas flows. Mechanisms by which the flow pattern changes from stratified flow to any of the other flow patterns considered were then described. Their theory suggested that the transition between annular and intermittent flows depends uniquely on the liquid level in the stratified equilibrium flow. They also suggested that the transition from intermittent to bubble regimes takes place when the turbulent fluctuations superimposed on the stratified equilibrium flow are strong enough to overcome the buoyant forces tending to keep the gas at the top of the pipe. By extending the Kelvin-Helmholtz theory for wave instability to the round pipe geometry, the condition for the transition between stratified and intermittent or annular flows was obtained. Some of the predictions of this analysis will be compared with the results of the present investigation in a later chapter. Also, for the sake of completeness, the mathematical derivations for the annular-wavy and annular-intermittent transition lines are presented in Appendix A. These lines were selected because of their relevance to the present study.

2.2 Diabatic Flow Studies

This type of flow encompasses both the condensation and boiling cases. The presence of heat transfer complicates the flow situation since the phase distribution as well as the velocities of the two phases change along the axis of the duct. As a result, different flow patterns are expected to exist between the inlet and the exit of the flow channel. Flow patterns should be correlated according to the local conditions at which they appear, rather than the average conditions such as is the case with adiabatic flow studies. This will, of course, introduce more complications into the design of the test section, test procedure, instrumentation, and data reduction.

In this presentation, the main emphasis is placed on the condensation studies. Only one investigation dealing with the flow patterns of a boiling fluid is presented just to show the similarity between the two types of flow in terms of flow patterns and methods of data presentation.

Zahn [15] visually studied the flow patterns of evaporating Freon-22 inside 0.46 in. I.D. horizontal tubes. The pressure, temperature, flow and heat load conditions covered were similar to those associated with the actual operation of a small air-conditioning coil. The observation area consisted of two specially fabricated double-pipe glass tube sections. Flow patterns similar to those observed in

adiabatic studies (e.g., wavy, slug, annular, and spray) were reported. New flow patterns were also identified such as the semi-annular which had an annular appearance with liquid film covering only the lower part of the tube. When plotting the flow pattern data on Baker's [5] map, most of the points occupied the area classified by Baker as "annular". The wavy flow data points scattered between the slug and annular flow areas. Due to this discrepancy, Zahn presented his data in a map using the vapor volumetric ratio

$$R = Q_v/(Q_\ell + Q_v) \tag{2.5}$$

and the Froude number

$$N_{FR} = \left|\frac{Q_\ell + Q_v}{A}\right|^2 gD \tag{2.6}$$

as coordinates. He recommended this map for prediction of boiling flow patterns under similar operating conditions.

The first attempt to study the two-phase flow patterns during condensation was made by Soliman [16] and the results were also reported in [17]. He visually and photographically observed the flow patterns of Freon-12 condensing inside a 0.5 in. I.D. horizontal tube. The test section used in the experimental analysis consisted of three separate double pipe counter flow condensers joined together by three observation sections. Flow patterns similar to those observed in [15] were reported, with the addition of the plug flow. The obtained data did not correlate well with Baker's

[5] map. Due to the lack of any standard method for data presentation, few maps were prepared using different co-ordinate systems. The most important one was generated using Baker's coordinates with the boundaries relocated to accommodate the data. Following this work Traviss and Rohsenow [18] studied the flow patterns of Freon-12 condensing in 0.315 in. I.D. horizontal tube. They reported data and descriptions for the spray, annular, semi-annular, and slug flow patterns. Wavy flow was not observed. Their description of the semi-annular flow pattern was similar to the description given in [16] and [17] for the annular-wavy flow. Traviss and Rohsenow [18] concluded that Baker's [5] map predicted their data fairly well. The author disagrees with this conclusion because of the lack of data for wavy flow and the questionable identification of semi-annular flow. A theory was developed by Traviss and Rohsenow for the annular to stratified flow pattern transition. The predictions of this theory will be compared with the results of the present investigation in a later chapter.

To investigate the effects of fluid properties and pipe diameter, Soliman [19] studied the flow patterns of Freon-12 and Freon-113 condensing inside three tubes with 0.1875, 0.5, and 0.625 in. inside diameters. Results were also reported in [20]. The descriptions on which basis the flow patterns were identified were mainly the same as those used in [16] and

[17]. Baker's [5] map again failed in predicting any of the data sets corresonding to any tube diameter and any condensing fluid. Most of the findings of this research effort will be referred to later in this thesis. Palen et al. [21] reported a study on the flow patterns of both water and n-pentane condensing inside a 0.87 in. I.D. horizontal glass tube. Although no data were presented, Palen et al. [21] reported that Baker's [5] map was found inadequate for condensation. Later, Breber et al. [22] explored the applicability of the theoretical predictions of Taitel and Dukler [14] to condensation. For this purpose, they used the data reported in [16], [18], [19], [21], and few other sources. Fair agreement resulted for the annular and wavy flows, and poor agreement for the slug flow. Breber et al. then suggested a simplified correlation for the prediction of condensation flow pattern which will be tested later with the results of the present investigation.

After reviewing the work available in the literature on flow patterns of condensing fluids, it was concluded that additional efforts are needed. Reported data are limited and further experiments are required to establish the effects of fluid properties and pipe diameter on the flow patterns and flow pattern correlations. The present experimental investigation is a first step towards achieving this goal.

CHAPTER 3

EXPERIMENTAL FACILITY

An experimental test facility was designed and constructed for the study of flow patterns of condensing steam inside horizontal tubes. Steam was selected as the test fluid because it is widely different in physical and transport properties from Freon-12 and Freon-113 to which most of the published data correspond. The present experiment was conducted using a test condenser a 0.527 in. I.D. inner tube. The following major requirements were satisfied in the design of the present test facility:

1. System is capable of providing flow pattern data at variable steam flow rates up to a maximum of 500 lb_m/hr.
2. System pressure varies according to steam mass flow rate; however, it does not exceed 50 psig.
3. In any test run, steam enters the test condenser with an adjustable amount of superheat and complete condensation can be achieved before the outlet.
4. At any steam flow rate, the cooling rate in the test condenser can be adjusted to any desirable value.
5. Proper instrumentation installed such that the flow conditions corresponding to each visual observation can be calculated.

6. Possible extension to other test fluids and other tube diameters with minimum modifications.

Detailed description is given below for the equipment used to satisfy the above objectives.

3.1 The Steam Circuit

Figure 3.1 shows a schematic diagram of the closed loop through which the test fluid (steam) was circulated. A general description is given here, while more details about the major components will be provided later in this chapter.

First, a controllable amount of steam was generated in the boiler from distilled water. Building steam at high pressure and temperature was used as the heat source. Generated steam was then passed through a superheater before entering the test condenser. The superheater is basically a 3.5 ft. long, double pipe heat exchanger with the test fluid flowing in the inner pipe while building steam is flowing counter currently in the shell. Copper tubing, 0.785 in. I.D. and 0.875 in. O.D. was used for the inner pipe and 1.505 in. I.D. and 1.565 in. O.D. was used for the outer pipe. The whole exchanger was covered on the outside by 2.5 in. thick fiberglass insulation. The flow of building steam into the superheater is controlled by a valve, thus providing some control on the degree of superheat of the test fluid. At the inlet and outlet of the test condenser

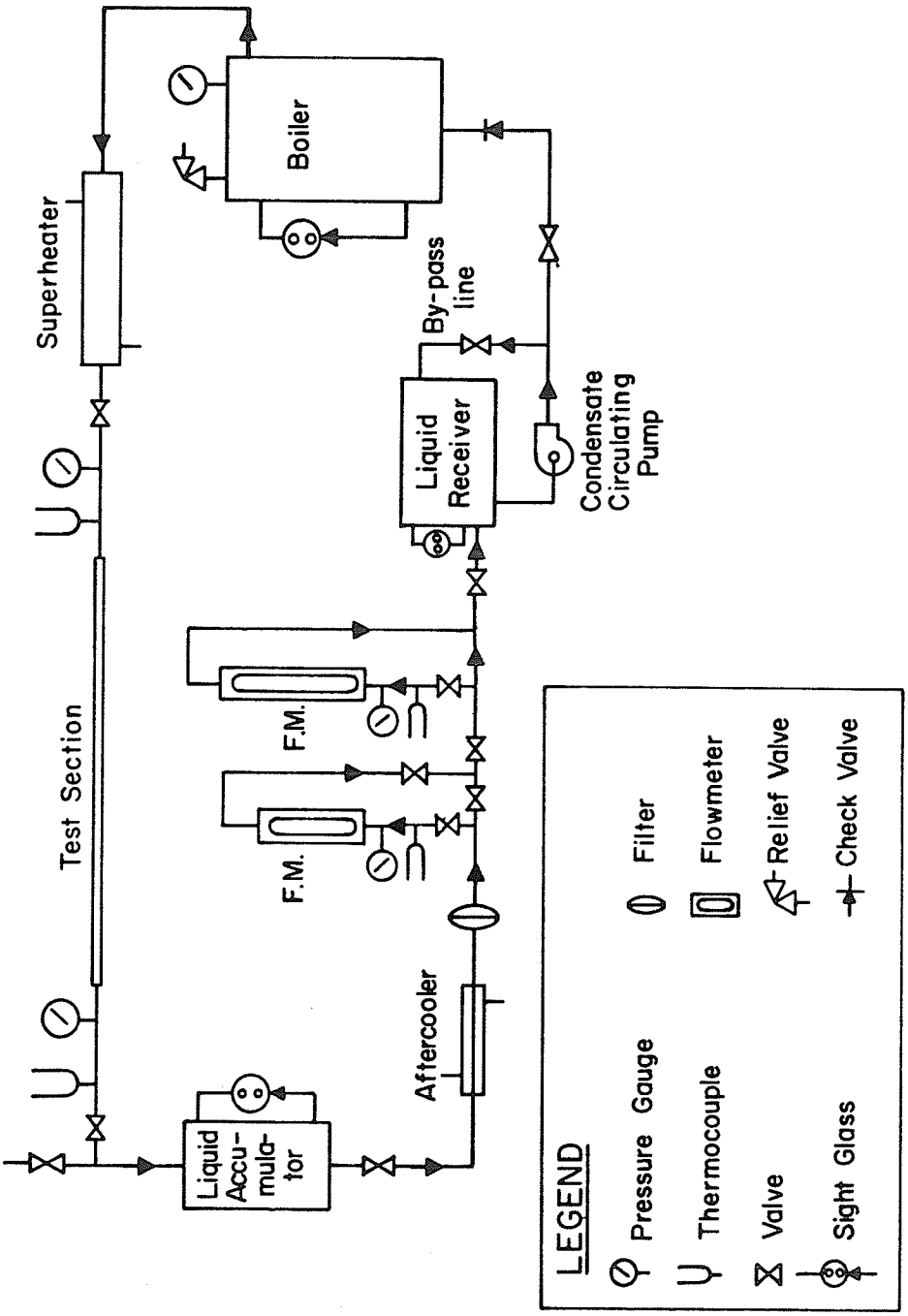

Fig. 3.1. Schematic flow diagram of the steam circuit.

the pressure was measured by Ashcroft Bourdon tube pressure gauges and the temperature was measured by 24 gauge, copper-constantan thermocouples. Complete condensation was achieved in the test condenser using water as the cooling medium. Downstream of the condenser, a liquid accumulator was installed to receive the condensate. This is basically an 11.2 gallon, copper tank, with a sight glass to show the level of liquid inside, and covered on the outside by 2.5 in. thick fiberglass insulation. The flow out of the liquid accumulator is controlled by a valve, and hence by adjusting the opening of this valve a steady liquid level can be achieved in which case the flows of condensate into and out of the accumulator would be equal. Thus, by measuring the rate of flow leaving the accumulator, the steam mass flow rate through the test condenser can be calculated. This was done by two precalibrated Brooks flow meters of the variable area type with ranges to 0.2 and to 1.0 gpm. Only one of these flow meters was used in any particular run depending on the flow rate. Because of the overlapping ranges, an accurate measurement of the flow rate is insured anywhere within the range 0.02 - 1.0 gpm. Immediately upstream of each flow meter the pressure and temperature were measured by a Bourdon tube pressure gauge and a copper-constantan thermocouple, respectively. These measurements are necessary for the evaluation of fluid properties at the flow meters.

Between the liquid accumulator and the flow meters, an after-cooler was installed to avoid flashing in the flow meters. After measuring the flow rate, the liquid then flowed into a liquid receiver installed at the suction side of the circulating pump. This receiver is 22.4 gallons in capacity and equipped with a sight glass. Its purpose is to ensure continuous and steady liquid supply to the circulating pump. This pump is a single speed, 3/4 HP centrifugal pump and it is required to drive the condensate back to the boiler to complete the circuit. Since different flow rates were used in the experimental course, the circulating pump was equipped with a by-pass line to control the net flow going back to the boiler. One of the requirements for steady state conditions in any test run was that the liquid level in the receiver tank remained steady.

The whole circuit was tested for leaks under vacuum and pressurized conditions. This was done to ensure the absence of air or any other non-condensable gases in the loop during the tests. The system proved to be leak proof within (-14 to 50 psig). Before the start of the experiment, the system was evacuated, then charged with steam, then re-evacuated.

3.1.1 The test condenser

Two test condensers were used in the course of this experiment, both having the same inside diameter for the

inner tube and the same total condensing length. The only difference is in the number of visual sections; four in the original design and five in the final design. These two designs are shown schematically in Fig. 3.2. Description is given here for only the initial design since there is no major difference between the two.

The initial test condenser consisted of four separate condensing units (labeled a,b,c, and d in Fig. 3.2a), each followed by a visual section (labeled A,B,C, and D). All condensing units were 4 ft long, double-pipe heat exchangers made of copper with steam flowing in the inner pipe and the cooling water flowing counter currently in the shell. The inner pipe was 0.527 in. O.D. and 0.625 in. O.D., while the outer pipe was 0.745 in. I.D. and 0.875 in. O.D. The small gap between the outer surface of the inner pipe and the inner surface of the outer pipe (0.06 in.) was selected to increase the velocity of the cooling water and consequently the heat transfer coefficient. This resulted in complete condensation in all test runs. All condensing units were covered on the outside by 2.5 in. thick fiberglass insulation.

Fig. 3.3 shows the construction details of one of the visual sections. It consists mainly of a 9 in. long, standard clear, high pressure glass tube supported on both ends by a stuffing box to prevent leakage. The glass tube was selected such that the inside diameter is close to 0.527

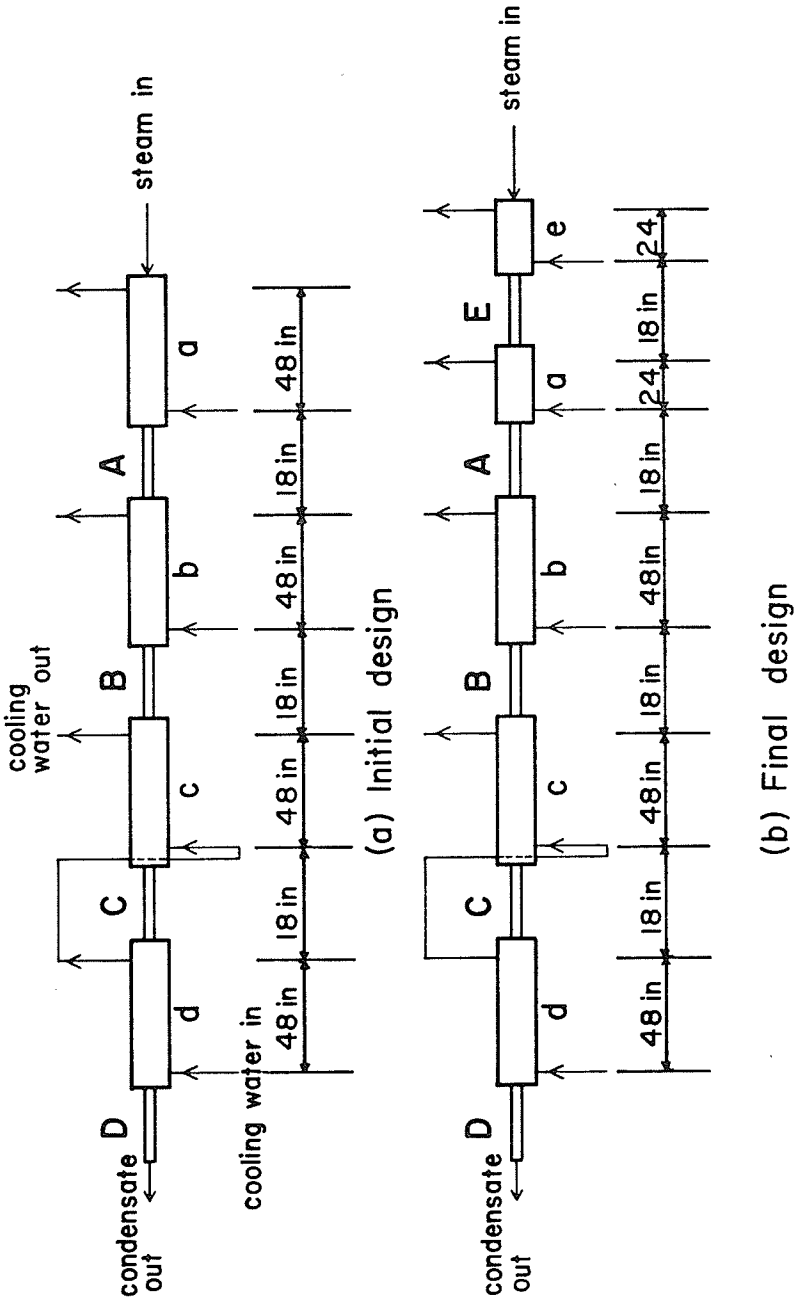

Fig. 3.2 Schematic diagram of test condenser.

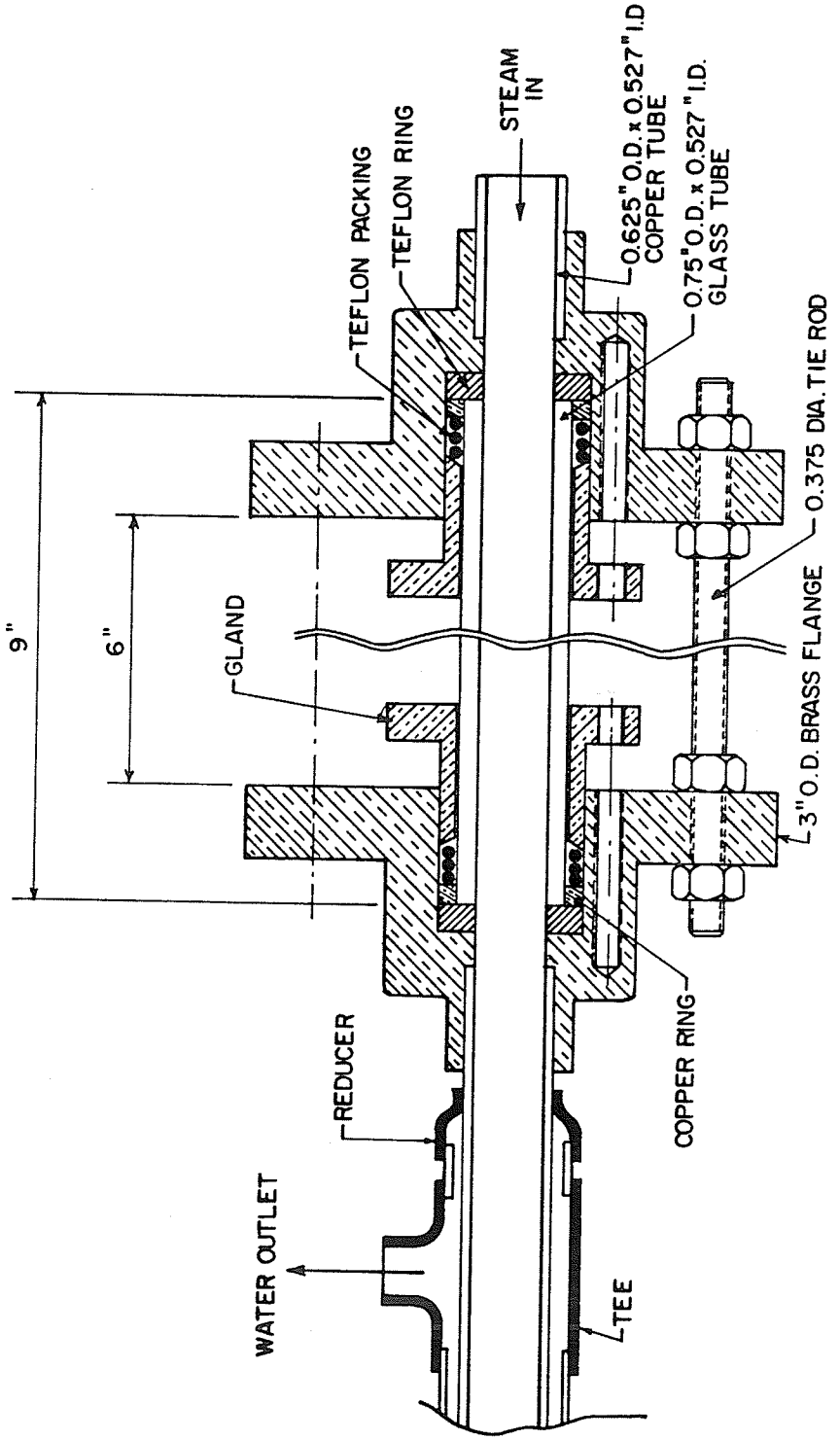

Fig. 3.3. Construction details of one visual section.

in. to avoid discontinuities in the steam passage. Precautions were also taken for coaxiality with the condensing units (e.g., the copper rings mounted at both ends of the glass tube, shown in Fig. 3.3). Teflon was used as packing in the stuffing boxes. The visual section was held together by three tie rods.

At both ends of the test section, an expansion joint was installed to absorb any thermal expansion. The whole test condenser was supported by a steel frame with design features to accommodate the addition of other test condensers in the future. Finally, the horizontality of the test condenser was checked by a survey transient.

3.1.2 The boiler

A boiler was designed and manufactured locally consisting mainly of an outer shell and an internal heating coil. The outer shell is 3 ft. I.D., 1.5 in. thick, 6 ft high, and made of galvanized iron. The heating coil was manufactured using a total of 330 ft. of commercial steel pipe (0.375 in. nominal schedule 40 standard), which was found to provide enough heat transfer surface. The coil was galvanized on the outside to avoid contamination and rust. A sight glass was installed to monitor the liquid level inside the boiler and a safety valve set at 50 psig was placed at the top to avoid excessive pressure build-up. The boiler was insulated

by 2.5 in. thick fiberglass. Rate of steam generation was controlled by regulating the flow of building steam. The boiler arrangement is shown schematically in Fig. 3.4.

3.2 The Cooling Water Circuit

The cooling system used in the present investigation is shown in Fig. 3.5. It is of the open-loop type and was designed to permit complete control on the coolant flow rate to each condensing unit in the test section. Tap water, used as the coolant, was collected in a 50 gallon surge tank with an overflow line to avoid flooding. The water was then circulated by a 10 horsepower turbine pump with a maximum capacity of 20 gpm and a maximum head of 460 ft. Downstream from the pump a by-pass line was used to control the cooling water flow rate into the test section. Four Brooks flow meters of the variable area type mounted in parallel, were used to measure the water flow rate. Maximum reading of all flow meters is 4.2 gpm. Flow meters I, II and III are connected to condensing units e, a, and b, respectively, while flow meter IV is connected to condensing units c and d. Check valves are mounted at the water outlet of each condensing unit to avoid flow reversal. Water leaving the condenser was then drained through a common line. The control of the water flow rate to each condensing unit was achieved by adjusting the opening of the valves installed

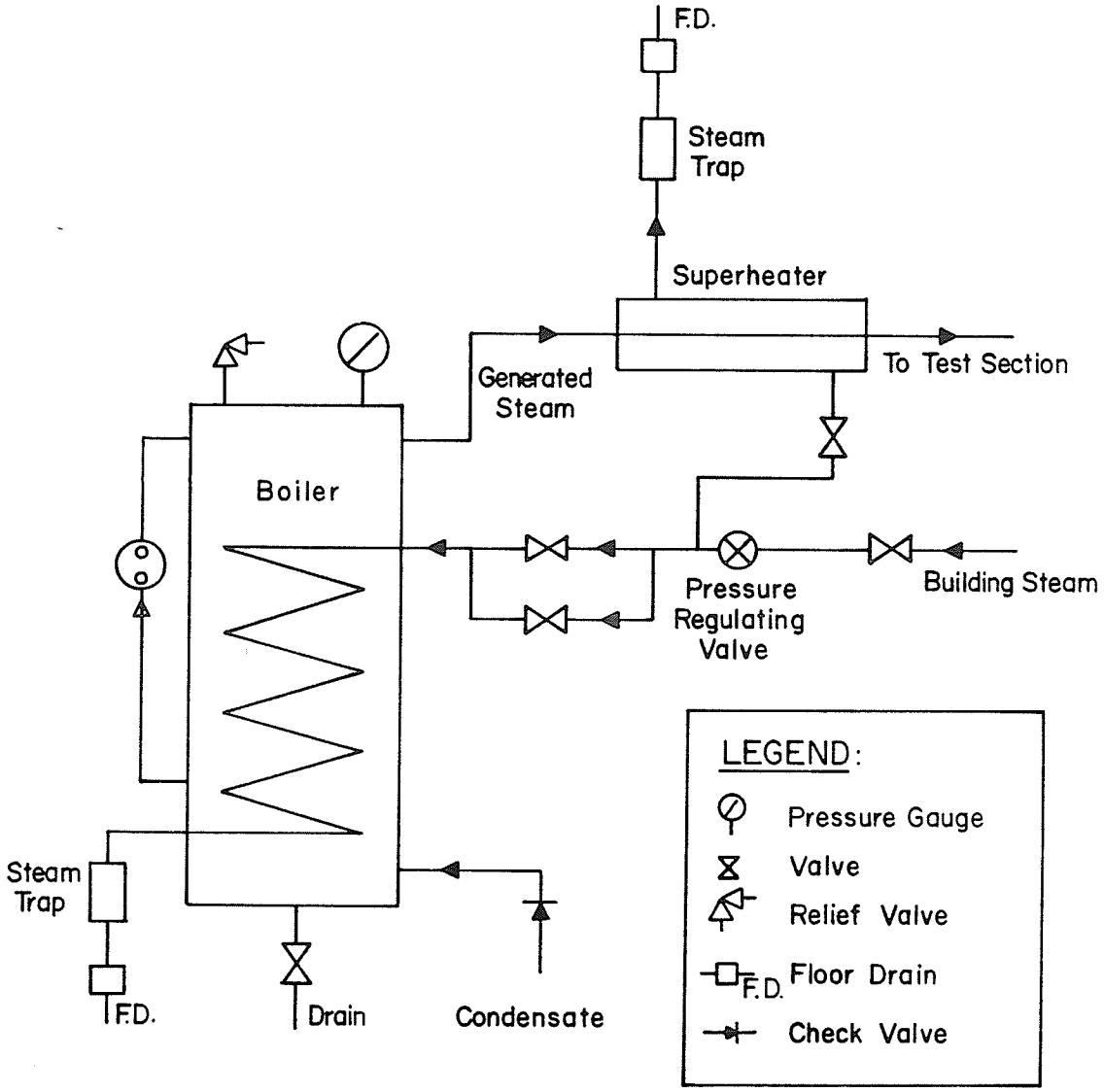

Fig. 3.4. Simplified diagram of the boiler arrangement.

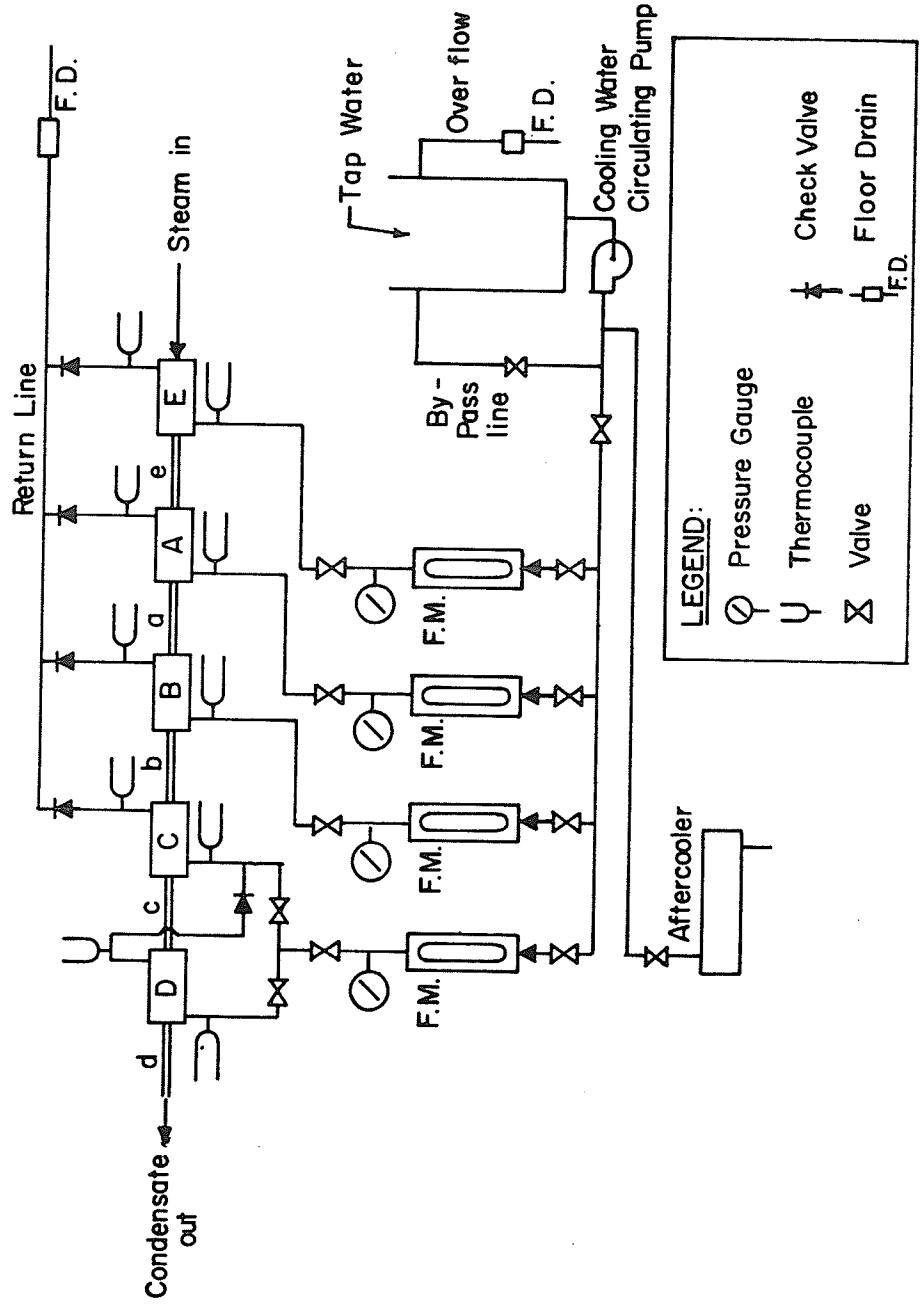

Fig. 3.5. Schematic diagram of the cooling water circuit.

before and after each flow meter. In addition, the water temperature was measured at the inlet and outlet of each condensing unit.

All flow meters and thermocouples were precalibrated before installation in the system. A Leeds and Northrup digital potentiometer (model 914) was used to measure the thermocouple outputs in °F.

3.3 Experimental Procedure

Several test runs were performed in order to cover a wide range of steam flow rates, inlet superheats, pressures and cooling rates. The procedure followed in each run is described in the following sub-sections:

3.3.1 Start up procedure

The steps taken to start up the experimental facility and to prepare for any test run are listed below in the order conducted:

1 - The potentiometer was turned on.

2 - Adjustable amount of building steam was allowed, after regulating its pressure by the regulating valve, to flow into the boiler.

3 - Cooling water surge tank was filled to the overflow level.

4 - The valve downstream from the liquid accumulator was closed.

5 - Cooling water circulating pump was turned on with its by-pass valve fully opened.

6 - Cooling water was allowed to flow gradually into the test condenser by partially closing the pump by-pass valve and adjusting the valves upstream and downstream from the flow meters.

7 - When steam started flowing into the condenser, the valve upstream of the superheater was opened.

8 - When the liquid accumulator became almost 3/4 full, the valve downstream from it was partially opened to allow the condensate to flow into the appropriate flow meter.

9 - The condensate circulating pump was turned on with its by-pass valve adjusted to keep a steady level in the liquid receiver.

10 - Continuous adjustments were made for the flow rate of building steam into the boiler and superheater, cooling water flow rates, condensate flow meter reading, and the condensate flow rate back to the boiler until steady state conditions were reached.

3.3.2 Steady state conditions

The criteria used for reaching steady state conditions was that the following readings remained unchanged for a period of at least 1/2 hour.

1 - Condensate levels in the liquid accumulator and liquid receiver.

2 - Pressures at the inlet and exit of test condenser.

3 - All temperatures on the steam and cooling water sides.

4 - Condensate flow meter as well as cooling water flow meters.

5 - Observed flow pattern in all visual sections.

Although the steady state conditions could be reached within two hours from start up, the system was run for at least three hours before any data or any flow pattern observations were recorded.

3.3.3 Recording of data

Before each test run the ambient temperature and the barometric pressure were recorded. After reaching steady-state conditions the following readings were recorded:

1 - Boiler pressure in psig.

2 - Building steam pressure after the regulating valve in psig.

3 - Test condenser inlet and exit gauge pressures in psig.

4 - Test condenser inlet and exit temperatures in °F.

5 - Cooling water inlet and exit temperatures for each condensing unit in °F.

6 - Condensate temperature upstream of the condensate flow meter in °F.

7 - Cooling water flow rate to each condensing unit in gpm.

8 - Condensate flow rate in gpm.

3.3.4 Observation of flow patterns

For each run, after establishing steady-state conditions, the flow patterns at the visual sections A,B,C,D, and E were carefully observed. A sketch and a full description of each observation were recorded.

CHAPTER 4

RESULTS AND DISCUSSION

4.1 Data Reductions

A total of 98 test runs were recorded during the present investigation. Runs 1 through 61 were carried out using the initial design of the test section, shown in Fig. 3.2a, while the rest of the runs correspond to the final design after the inclusion of an additional visual section, as shown in Fig. 3.2b. In each run, the test fluid flow rate, cooling water flow rates, and inlet superheat were individually adjusted to the desired values. There was no control on the pressure of the system, the magnitude of which was dependent on the mass flow rate of the test fluid. Ranges of operating conditions covered in this investigation are listed in Table 4.1. Values of inlet superheat were calculated as the difference between inlet temperature and the saturation temperature corresponding to inlet pressure. Working pressure will be defined later.

The raw data recorded during the experimental course were reduced on an IBM 370/168 digital computer using FORTRAN IV language. The program first calculates the rates of heat loss by the steam and heat gain by the cooling water over the whole test section. Based on these values, the percentage heat balance error is calculated as [(rate

Table 4.1: Ranges of Operating Conditions

Number of test runs	98
Number of observations	174
Working pressure P, (psia)	16.0-35.6
Mass velocity G, $(lb_m/hr\text{-}ft^2) \times 10^{-4}$	3.15-18.17
Inlet superheat (°F)	8.6-50.0
Quality x at visual sections	0.01-0.7
Average rate of heat transfer (Btu/hr) $\times 10^{-4}$	4.88-30.15

of heat loss by steam-rate of heat gain by cooling water)/ rate of heat loss by steam] x 100. Only test runs with a heat balance error within $\pm$ 10% were recorded, while the few runs which did not meet this requirement were rejected. In addition, it should be pointed out that 73 of the total 98 test runs had heat balance errors within $\pm$ 5%.

Calculation then proceeded to the evaluation of operating conditions for the acceptable runs. The working pressure was taken as the average of the inlet and outlet pressures, and the saturation temperature was obtained corresponding to this pressure. All properties, such as liquid density ρ_ℓ, vapor density ρ_V, liquid viscosity μ_ℓ, vapor viscosity μ_V , liquid surface tension σ .... etc., were evaluated at the working pressure and the corresponding saturation temperature. Operating conditions for all acceptable test runs are tabulated in Appendix B.

Flow pattern parameters corresponding to each visual observation were calculated based on the local quality and the properties evaluated earlier. As was mentioned in the previous chapter, the system was designed to have superheated steam at the inlet of the condenser, and subcooled liquid at the outlet visual section D, (Fig. 3.2). Considering the initial test section design, shown in Fig. 3.2a, the quality at visual sections A,B, and C were calculated from a simple heat balance on condensing units a,b, and c,

respectively. If the calculated quality at any visual section was less than zero, indicating a subcooled condition, then no flow pattern parameters were evaluated at this visual section. This situation occurred consistently at visual section C, and occasionally at visual section B. A similar calculation procedure was followed for the final test section design, shown in Fig. 3.2b. Details of the calculations of heat balance, operating conditions, and flow pattern parameters for one arbitrary run are provided in Appendix C. Also, a complete listing of calculated flow pattern parameters for all test runs is given in Appendix D.

The situation where a two-phase flow pattern was observed at a certain visual section, while the heat balance indicated a subcooled condition there deserves some discussion. This is important since this situation prevailed for all the slug, plug, and stratified flow pattern observations. All these flow patterns occurred in the present experimental study, but were not possible to correlate because the heat balance indicated a corresponding subcooled condition. One possible reason for this apparent discrepancy is that our heat balance approach is based on the hypothesis of thermodynamic equilibrium between the two phases, which may not be the case in reality. This assumption was used in all flow pattern studies reported in the literature. Due to the high speed of the flow, the vapor and the liquid may exist at

different temperatures, such that the average enthalpy of the mixture is less than the enthalpy of saturated liquid. As a result, the heat balance might result in subcooled conditions at a visual section where both liquid and vapor were observed. A second reason is the inequality of the rates of heat gained by cooling water and heat lost by steam, due to inescapable experimental errors. Because of this inequality, the rate of heat gain by water in each of the condensing units was adjusted as shown in the sample calculation of Appendix C. Naturally, this introduces some uncertainty in the values of quality at all visual sections. By keeping the heat balance error with $\pm$ 10%, this uncertainty was found to be small for the range of qualities considered in this investigation, and reported in Table 4.1. However, if the quality is extremely low, such as the anticipated case for the slug, plug, and stratified flow patterns, then this small uncertainty can be large enough to change the calculated state of the mixture from saturated to subcooled conditions. For the above two reasons, it was decided not to report flow pattern data for these three flow patterns since experimental accuracy cannot be ensured.

4.2 Flow Patterns

Six major and two transitional flow patterns were visually identified at the different observation sections.

The following descriptions were used in the present study to identify the different patterns:

Spray flow: the liquid phase is entrained by the vapor in the form of droplets. No liquid film can be observed around the tube. The flow appeares as a fog travelling at a very high speed. (plotted as x).

Spray-Annular flow: an unstable liquid film appears around the tube, but is swept away occasionally by the high speed vapor. Otherwise, the flow still has the same appearance of the spray flow. (plotted as ⊗).

Annular flow: a liquid film covers the whole circumference of the tube in the form of a ring, while the vapor is flowing in the core. Part of the liquid phase might be entrained within the vapor. (plotted as ●).

Annular-Wavy flow: the whole circumference of the tube is covered with liquid with a thick stratum at the bottom. The height of this stratum does not exceed half the radius of the tube. Vapor is still flowing in the core. (plotted as ◍).

Wavy flow: most of the liquid is flowing at the bottom of the tube and the vapor at the top with a wavy interface. A thin liquid film is still covering the upper part of the tube. The height of liquid at the bottom exceeds half the radius of the tube, but in all the observations was less than the full radius. In some

cases slugs appeared, but their frequency was as low as three to four slugs per minute. The flow was still classified as wavy in these cases since the appearance of these slugs occupied a minor portion of observation time. (plotted as 0).

Slug flow: liquid flows at the bottom and vapor at the top with a wavy interface. Waves grow large to form slugs touching the top of the tube. The frequency of these slugs is high enough to make them appear during a major part of observation time. (Data from other references plotted as ▲).

Plug flow: liquid flows as a continuous phase with the vapor in the form of large bubbles (or plugs) appearing in the upper part of the tube.

Stratified flow: liquid flows at the bottom and the vapor at the top with a smooth interface. This flow pattern existed mainly at the exit of the test section during runs with small flow rates.

Fig. 4.1 shows schematic diagrams of the above flow patterns.

4.3 Data Representation and Discussion

The main objective of this presentation is to study the suitability of different maps and correlations proposed in the literature for the prediction of two-phase flow

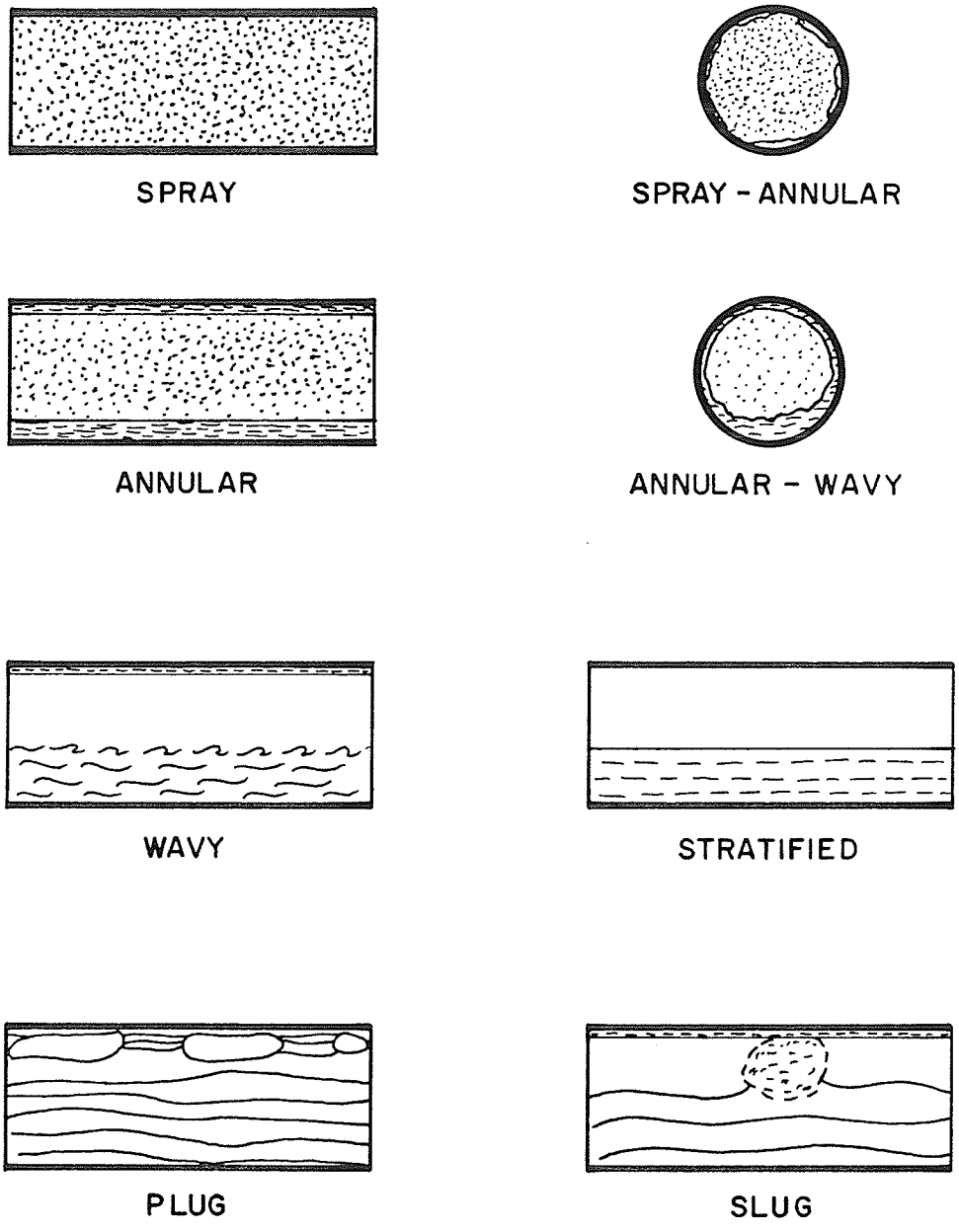

Fig. 4.1. Schematic diagrams of the flow patterns observed.

patterns of condensing fluids. Special attention will be directed to the influence of fluid properties on the location of transition lines between different flow regimes. Present data, as well as others reported in the literature, will be used to achieve these objectives. No attempt will be made here to generate new correlations.

4.3.1 Comparison with experimental correlations

Baker's [5] map is one of the most widely known correlations for two-phase flow patterns in the literature. Since this map was developed from data of different fluids and different tube diameters, it is expected that the transition lines of this map are, at least within limits, independent of fluid properties and tube diameter. Figure 4.2 shows a reproduction of Baker's [5] map with the present data plotted on it. The different areas on the map are marked according to Baker's predictions, and the key to the symbols used for plotting experimental points is given in Sec. 4.2. From Fig. 4.2, we can easily observe the following:

a) All the data of spray and spray-annular flow patterns appear in the annular flow area of the map.

b) All annular flow data are located in that same area on the map.

c) Most of the annular-wavy and wavy data points appear in the annular and slug areas of the map.

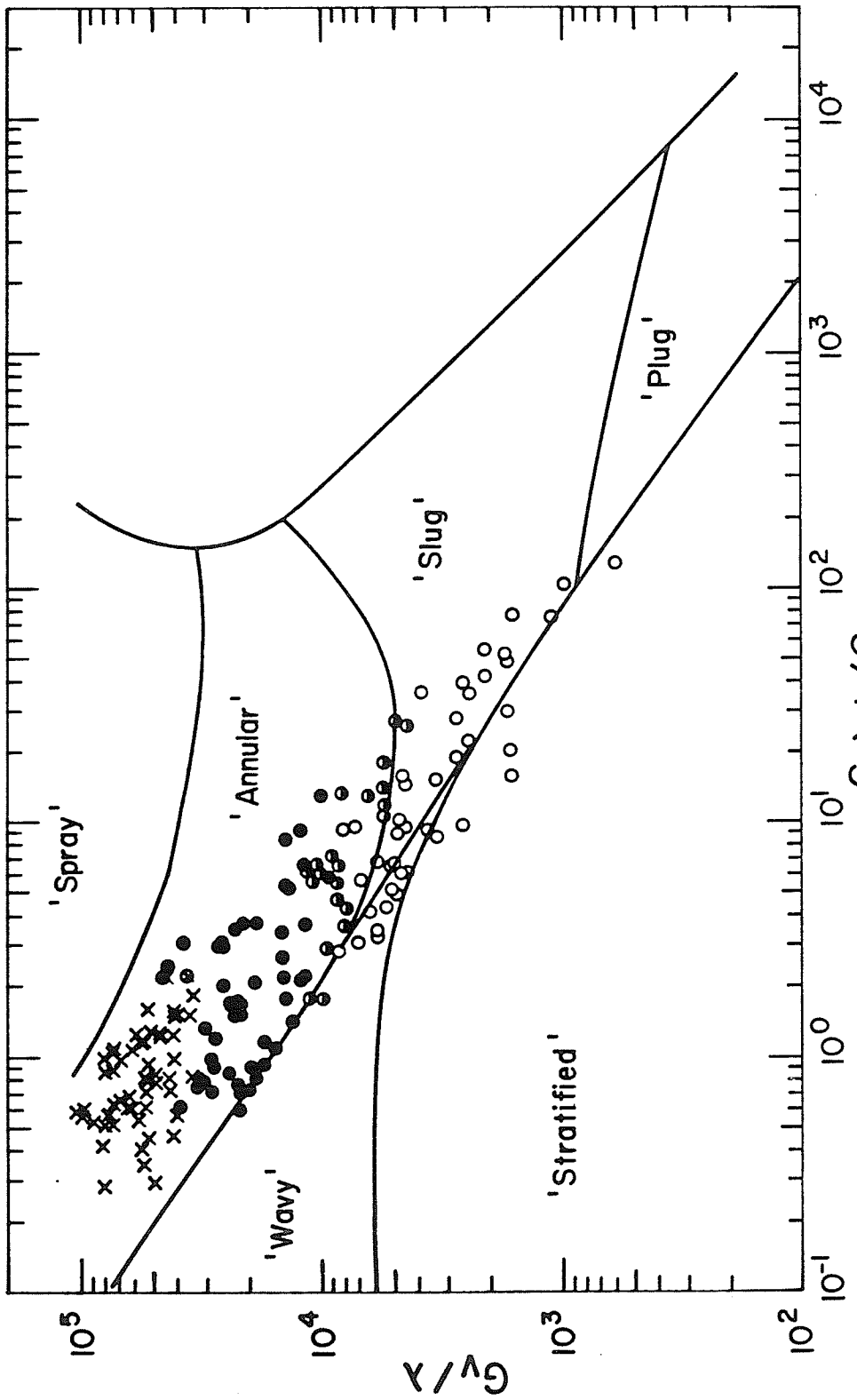

Fig. 4.2 Present data plotted on Baker's [5] map.

Based on the above observations it is fair to state that Baker's map failed in predicting the present experimental data. Similar conclusions were reported by Soliman [16], [19], Soliman and Azer [17], [20], and Palen et al. [21] for data of different tube diameters and different condensing fluids, which places the adequacy of this map for condensation in serious doubt. It should be pointed out also that disagreement with this map is not mainly due to inaccuracies in the locations of transition lines, but rather due to the improbable relative location of different areas. To explain this point, a run was selected from the present results and its path during condensation was traced on the map. The result is shown in Fig. 4.3. For this run, Baker's map predicts this sequence of flow patterns: Wavy-Annular-Slug-Stratified, while the experiment resulted in annular followed by wavy flows. As a matter of fact, the sequence of wavy followed by annular is impossible during condensation, and was never observed in the present investigation. The result of this comparison confirms similar conclusions drawn in [19], [20], and [21].

Soliman [19] and Soliman and Azer [20] proposed a map for the flow patterns of condensing fluids inside horizontal tubes based on their data of condensing Freon-12 and Freon-113 inside three different tube diameters. They used Baker's [5]

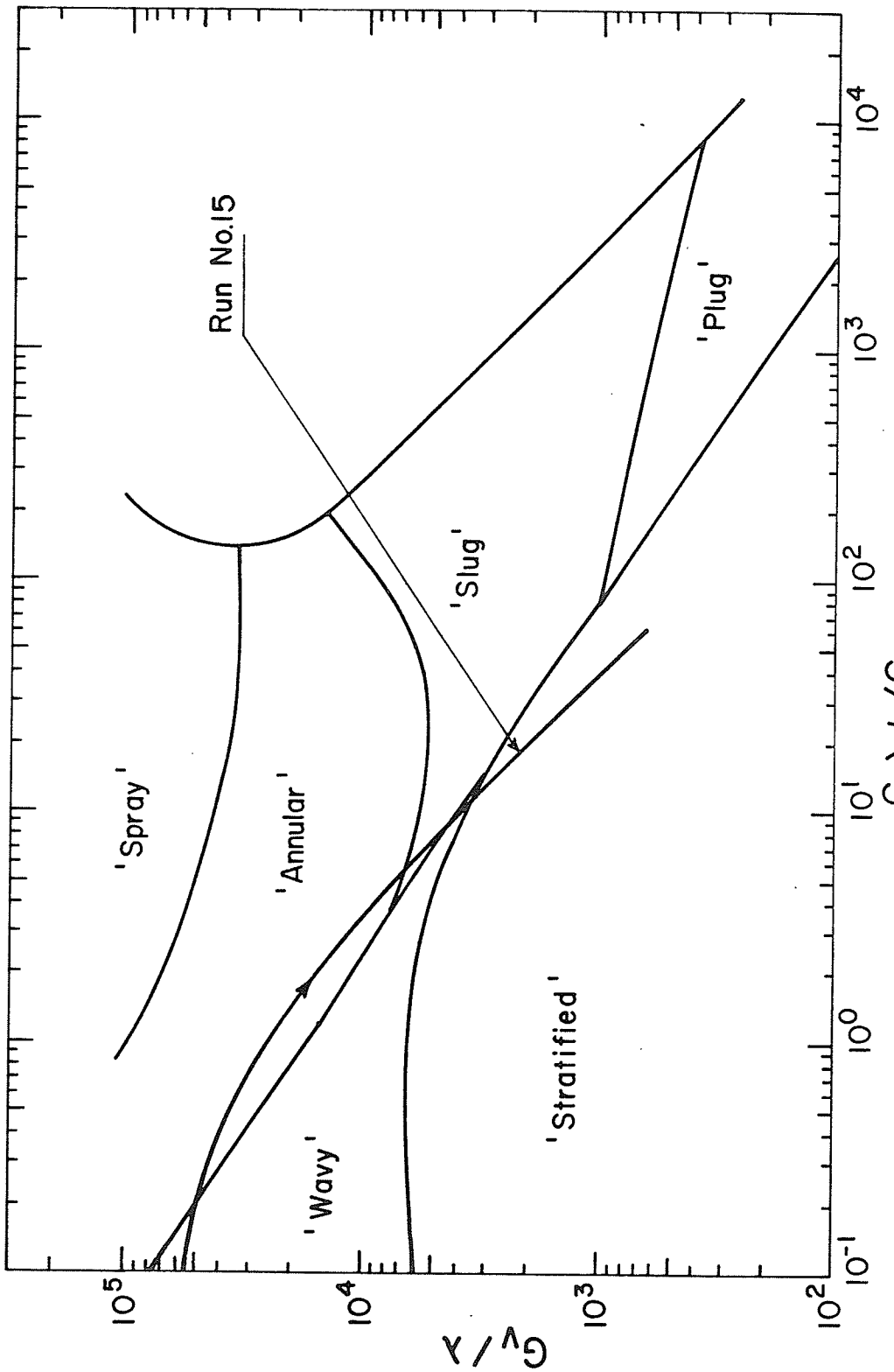

Fig. 4.3 Comparison of Run No. 15 with Baker's [5] map.

coordinates and relocated the different transition lines to fit their experimental data. This map is shown in Fig. 4.4 with the data of the present investigation superimposed on it. Before drawing any conclusions from this figure, it is important to quote the following description for the semi-annular flow from reference [19]: "Semi-annular flow: the flow had an appearance similar to the annular flow except the film thickness did not cover the entire periphery. A small portion of the upper half of the tube appeared dry while the liquid film thickness increased in the downward circumferential direction with the maximum film thickness being at the bottom." Although this flow pattern was not observed in the present investigation, based on the above description, it should not be viewed as fundamentally different from the annular flow pattern. Keeping this in mind and going back to Fig. 4.4 we notice a very good agreement between the map and the present data for the spray and annular flow patterns and a fair agreement for the wavy flow pattern. This agreement is remarkable given the fact that steam used in the present study is widely different in properties from Freon-12 and Freon-113 used in generating the map shown in Fig. 4.4 As a result, it is concluded that while Baker's [5] map proved inadequate, Baker's coordinates might be capable of absorbing the influences of fluid

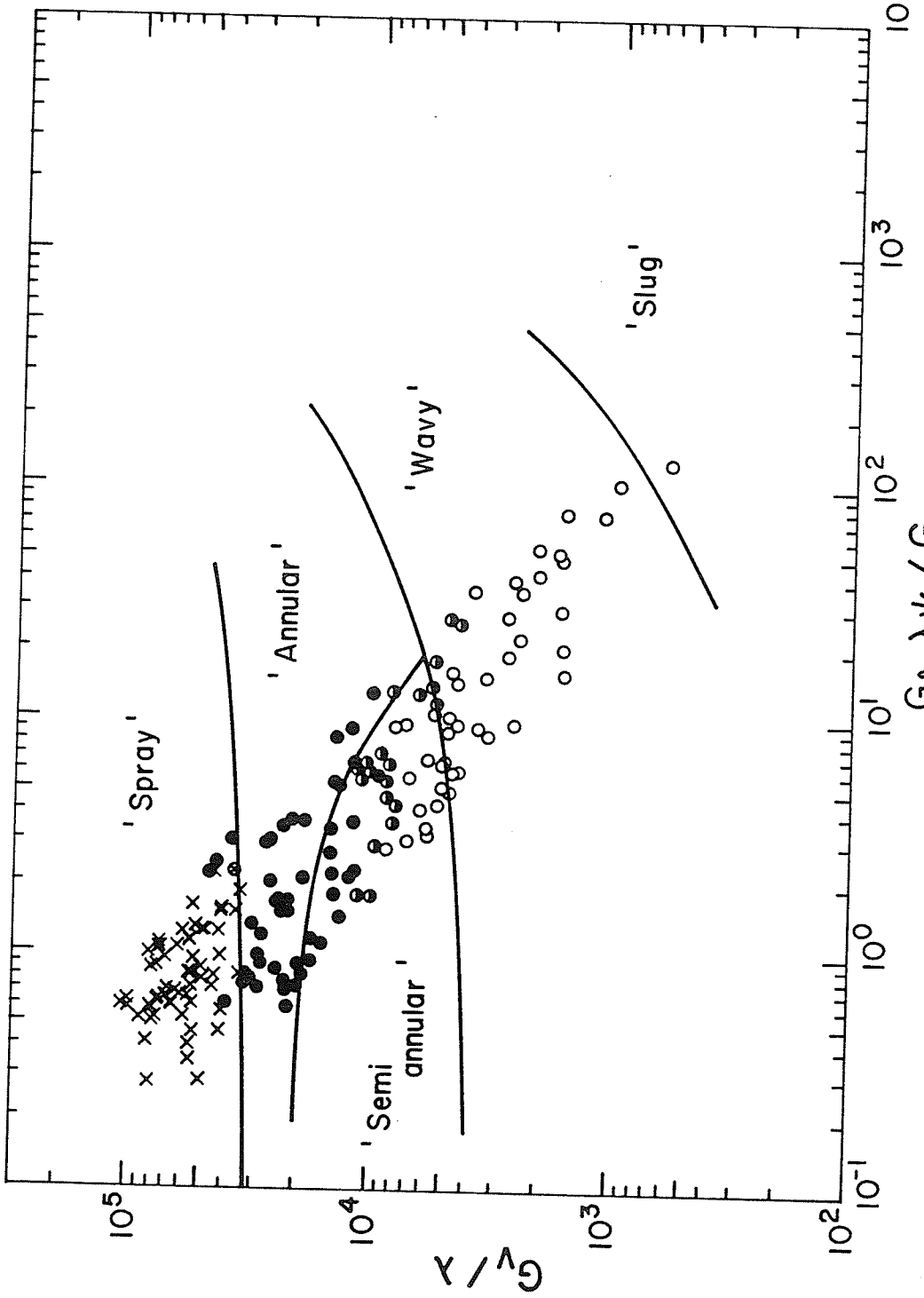

Figure 4.4 Present data plotted on a map proposed by Soliman [19] using Baker's [5] coordinates.

properties and tube diameter over a fairly wide range. Of course, more data especially for large tube diameters, (I.D. $\geq$ 1 in.) is needed to support this conclusion.

Another correlation which resulted from the studies [19], and[20] is a flow pattern map using V_ℓ and $(1 - \alpha)/\alpha$ as coordinates. Void fraction α was adopted because it characterizes the two-phase flow patterns in such a way that each flow pattern is associated with void fractions of a certain range. The liquid-phase velocity V_ℓ was defined as:

$$V_\ell = \frac{(1 - x)G}{(1 - \alpha)\rho_\ell} \quad . \tag{4.1}$$

The void fraction α was not measured in [19], and [20], but its value was calculated from the following semi-empirical formula developed by Smith [23]:

$$\alpha = \left\{ 1 + \frac{\rho_V}{\rho_\ell} K \left(\frac{1}{x} - 1\right) + \frac{\rho_V}{\rho_\ell} (1 - K)\left(\frac{1}{x} - 1\right) \left[\frac{(\rho_\ell/\rho_V) + K\left(\frac{1}{x} - 1\right)}{1 + K\left(\frac{1}{x} - 1\right)}\right]^{1/2} \right\}^{-1} \quad . \tag{4.2}$$

Where K is an empirical coefficient. A value of K = 0.4 was obtained by Smith [23] to give the best fit between theory and experiment. The flow pattern map by Soliman

[19] and Soliman and Azer [20] is shown in Fig. 4.5 with the data of the present investigation, calculated based on equations (4.1) and (4.2), superimposed on it. The agreement is very good, considering the fact that all transition lines represent transition zones of finite width. This fine agreement supports the hypothesis in [19], and [20] that V_ℓ and α can serve as parameters for the construction of a generalized flow pattern map for condensation.

Another well known two-phase flow pattern correlation is the map developed by Mandhane et al. [12], using superficial liquid velocity and superficial gas velocity as coordinates. As was mentioned earlier in Chapter 2, the transition lines of this map were developed from a wide base of experimental data (adiabatic, two-phase, two-component) corresponding to different tube diameters and gas-liquid combinations. Most of the data used however was for air-water mixtures. This map is shown in Fig. 4.6 with the data of the present investigation superimposed. Agreement is good. However, before making final conclusions about the applicability of this map, it was decided to test it with data of other fluids, while keeping the tube diameter almost unchanged. This test should explore the influence of fluid properties on the transition lines, which was claimed insignificant by Mandhane et al. [12]. The comparisons with

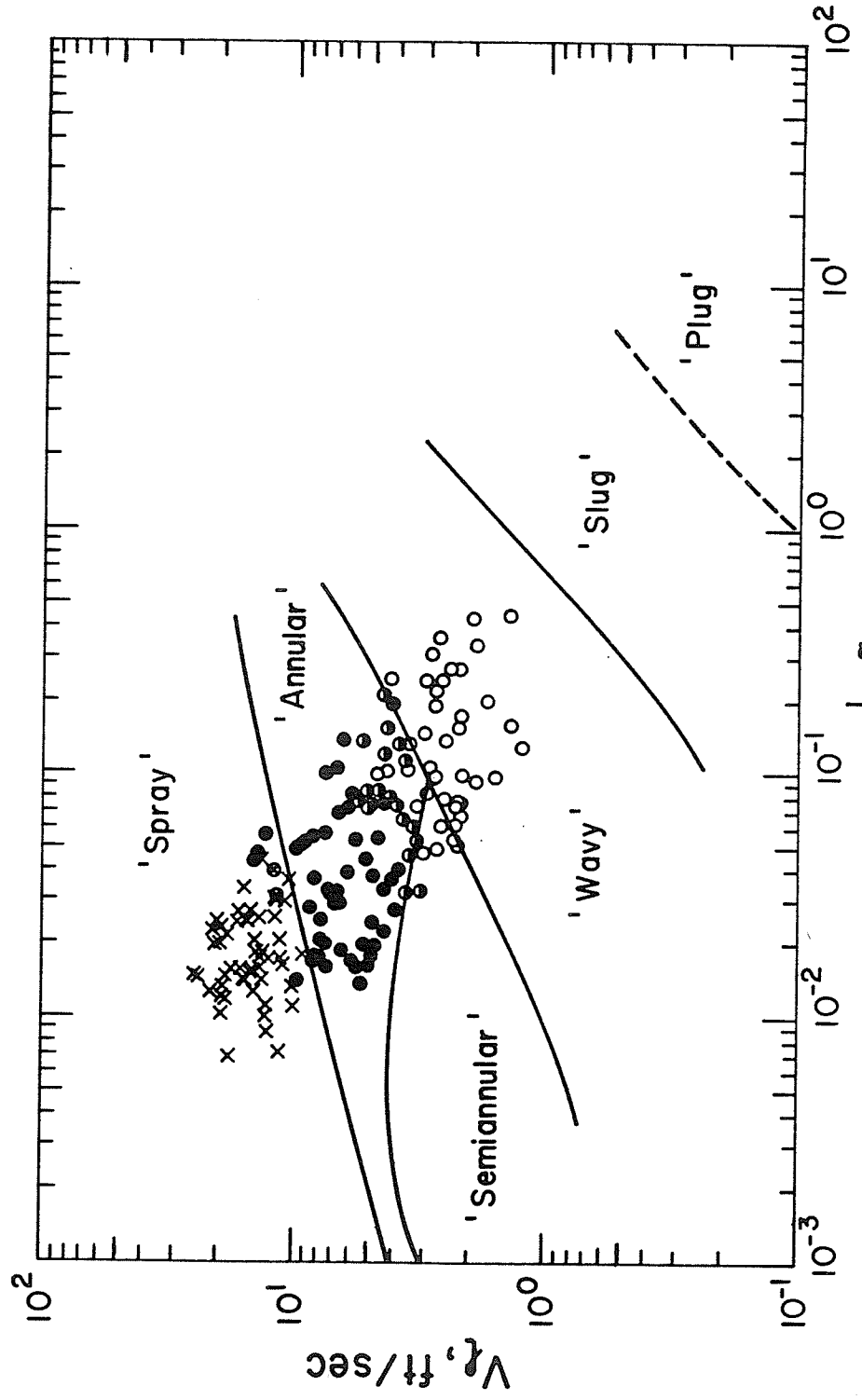

Fig. 4.5 Present data plotted on a map proposed by Soliman [19] using V_ℓ and $(1-\alpha/\alpha)$as coordinates.

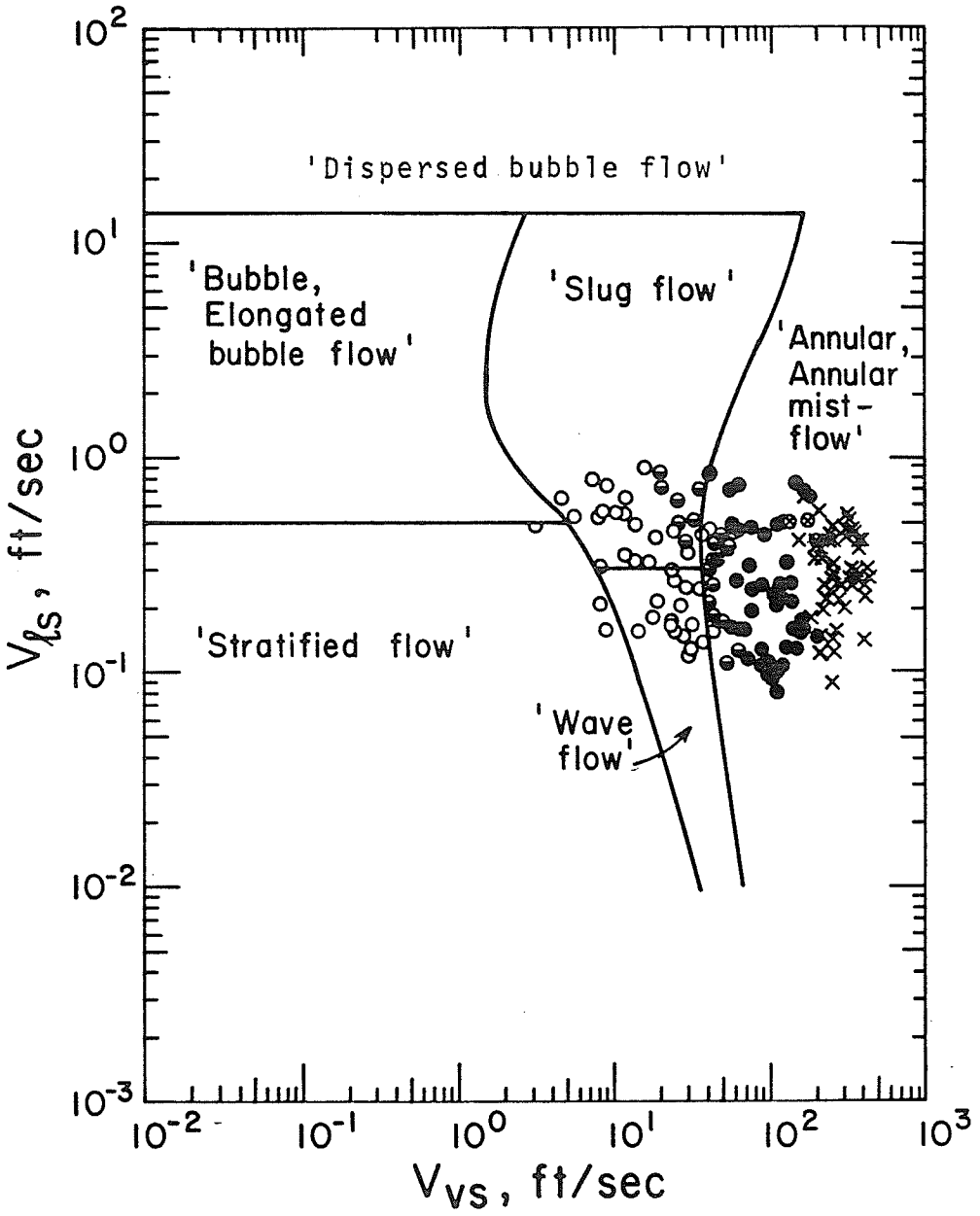

Fig. 4.6 Present data plotted on the map by Mandhane et al. [12].

flow pattern data of condensing Freon-113 and Freon-12 are shown in Figs. 4.7 and 4.8, respectively. Both data sets, reported by Soliman [16] and [19], correspond to a tube diameter of 0.5 in. which is close to the present tube diameter. As was mentioned earlier in this chapter, the semi-annular flow for Freon-12 and Freon-113 is not fundamentally different from the annular flow. For this reason it was decided to include the semi-annular observations with the annular flow. This approach will be used consistently whenever any proposed correlation will be tested against data reported in [16] and [19]. Figures 4.7 and 4.8 show very clearly that the transition lines of the map by Mandhane et al. [12] have to be considerably shifted in order to successfully predict the experimental data. This indicates that these transition lines are strongly influenced by fluid properties, contrary to the claim by Mandhane et al. The inadequacy of assuming that the $V_{\ell s}$ - V_{vs} coordinate maps are independent of fluid properties was also pointed out by Taitel and Dukler [14]. One reason for the good agreement resulting in Fig. 4.6 can be due to the fact that most of the data used by Mandhane et al. [12] in preparing their map correspond to air-water mixtures close to atmospheric conditions. The ratio (ρ_ℓ/ρ_V) for such mixtures would, of course, vary depending on the exact conditions; however, an

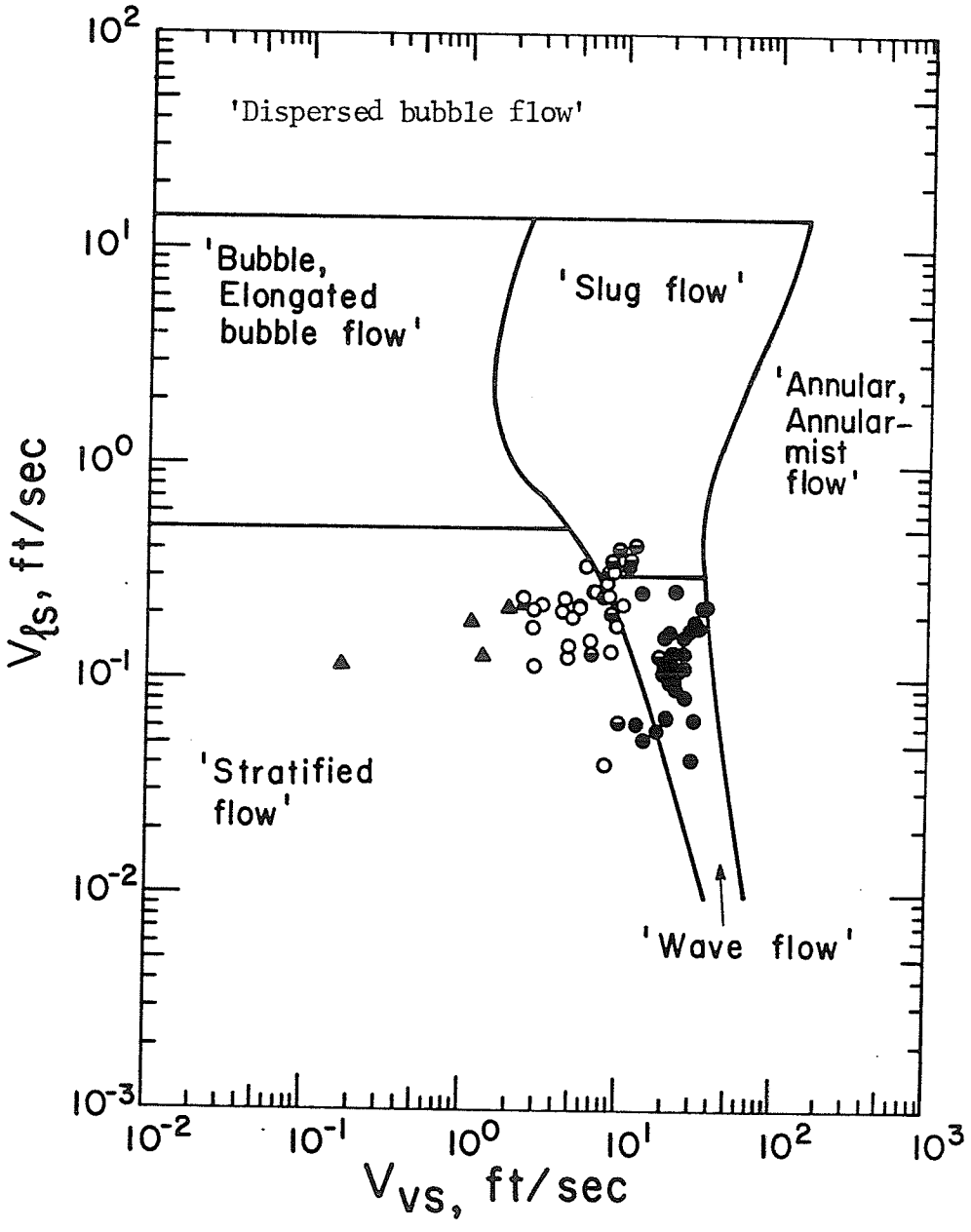

Fig. 4.7 Soliman's [19] data of Freon-113 condensing inside a 0.5 in. horizontal tube plotted on the map by Mandhane et al. [12].

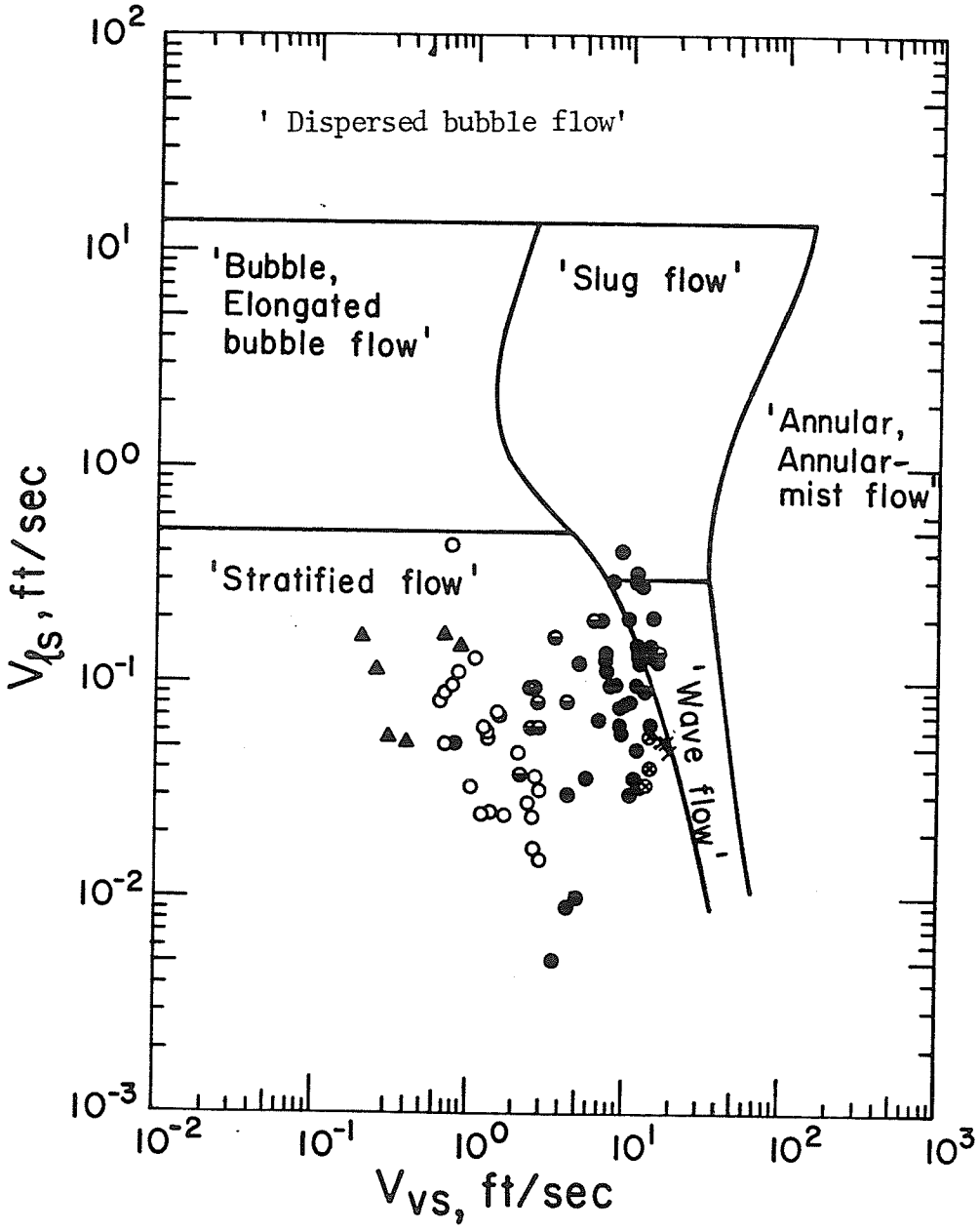

Fig. 4.8 Soliman's [16] data of Freon-12 condensing inside a 0.5 in. horizontal tube plotted on the map by Mandhane et al. [12].

average value for this ratio would be around 1000. Also the average values of (ρ_ℓ/ρ_V) for the data of steam, Fig. 4.6), Freon-113, Fig. 4.7, and Freon-12, Fig. 4.8 are 1150, 145, and 28, respectively. The fact that (ρ_ℓ/ρ_V) for steam in the present study has a value close to that for air-water mixtures [12] can be one of the reasons for the good agreement in Fig. 4.6.

4.3.2 Comparison with theoretical correlations

The investigation of the criteria governing the transitions between different two-phase flow patterns on a theoretical basis is an extremely difficult problem. This is due to the immense number of relevant parameters involved and the complexity of phase distributions existing during the flow. As a result, only few studies were reported in the literature with many simplifying assumptions adopted by the authors to facilitate the solution. Comparisons are made here between the experimental results of the present investigation as well as others reported in the literature and some of these theoretical predictions.

Traviss and Rohsenow [18] postulated that the Froude number is one of the controlling non-dimensional groups governing the transition between flow patterns that are not stratified (spray and annular) and flow patterns that are predominantly stratified (wavy, slug, and plug). Froude

number is a measure of the ratio of inertia forces and gravitational forces. Following a theoretical approach they developed the following equations for the transition line between the two groups of flow patterns:

$$N_{RE_\ell} = 1.38\ N_{GA}^{0.31}\ N_{FR_\ell}^{0.68}\ [F(X_{tt})]^{-0.94}, N_{RE_\ell} < 50 \quad (4.3a)$$

$$N_{RE_\ell} = 0.474\ N_{GA}^{0.34}\ N_{FR_\ell}^{0.68}\ [F(X_{tt})]^{-1.02}, 50 < N_{RE_\ell} < 1125 \quad (4.3b)$$

$$N_{RE_\ell} = 0.0442\ N_{GA}^{0.44}\ N_{FR_\ell}^{0.88}\ [F(X_{tt})]^{-1.33}, N_{RE_\ell} > 1125 \quad (4.3c)$$

where

$$N_{RE_\ell} = \frac{G(1-x)D}{\mu_\ell} \equiv \text{Reynolds number of the liquid,} \quad (4.3d)$$

$$N_{GA} = \frac{gD^3}{\nu_\ell^2} \equiv \text{Galileo number of the liquid,} \quad (4.3e)$$

$$F(X_{tt}) = 0.15\ [X_{tt}^{-1} + 2.85\ X_{tt}^{-0.476}]\ , \quad (4.3f)$$

$$X_{tt} = \left(\frac{\mu_\ell}{\mu_V}\right)^{0.1} \left(\frac{1-x}{x}\right)^{0.9} \left(\frac{\rho_V}{\rho_\ell}\right)^{0.5} \quad (4.3g)$$

$\equiv$ Lockhart and Martinelli [2] parameter,

and N_{FR_ℓ} is the Froude number of the liquid film.

Based on their experimental data of Freon-12 condensing inside a 0.315 in. horizontal tube they concluded that criterion (4.3) defines the transition at a constant value of Froude number, $N_{FR_\ell} = 45$. Equations (4.3b) and (4.3c) are plotted in Fig. 4.9 using N_{RE_ℓ} and X_{tt} as coordinates. The Galileo number was calculated from equation (4.3e) using the average saturation temperature and the inside diameter of the test section. The discontinuity appearing in the boundary line is due to the use of two different equations. Data of the present investigation are plotted in Fig. 4.9 with values of N_{RE_ℓ} and X_{tt} for all the data points calculated from equations (4.3d) and(4.3g), respectively. Equations (4.3b and c) succeeded in separating the annular and spray (not stratified) from the wavy (predominantly stratified) data points. The high accuracy obtained supports Traviss and Rohsenow [18] postulation. The constant value of $N_{FR_\ell} = 45$, which was obtained from their flow regime data on Freon-12, agrees well with the present data of steam. This implies that generality also can be claimed. However, before drawing final conclusions, it is necessary to explore the applicability of this criterion on data of other fluids with the same diameter. Data of Freon-12 and Freon-113 condensing inside 0.5 in. diameter tube, reported by Soliman [16] and [19], are plotted in Figs. 4.10 and 4.11, respectively. Equations (4.3b) and (4.3c) are also plotted on both figures

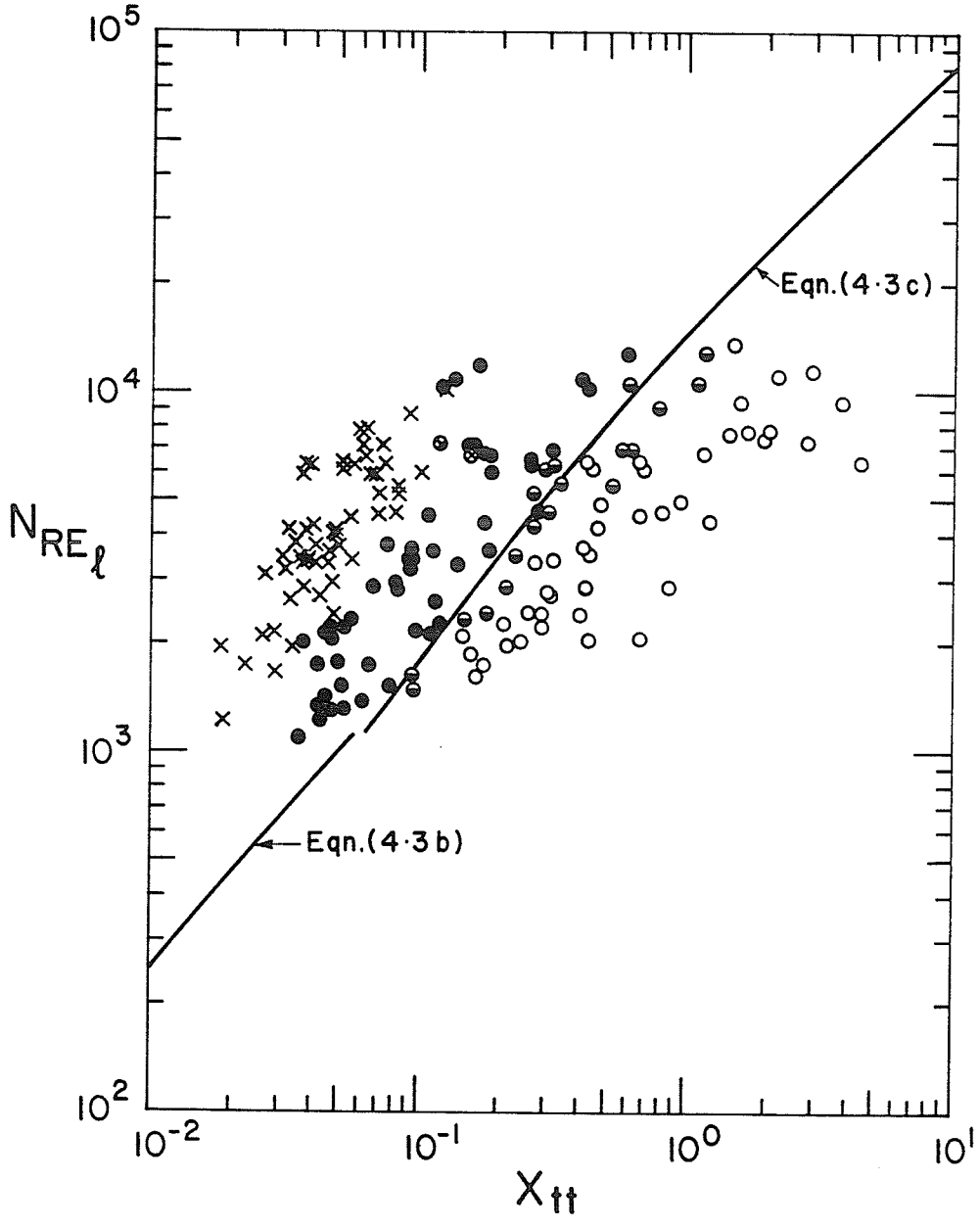

Fig. 4.9 Comparison between present data and the theoretical prediction of Traviss and Rohsenow [18].

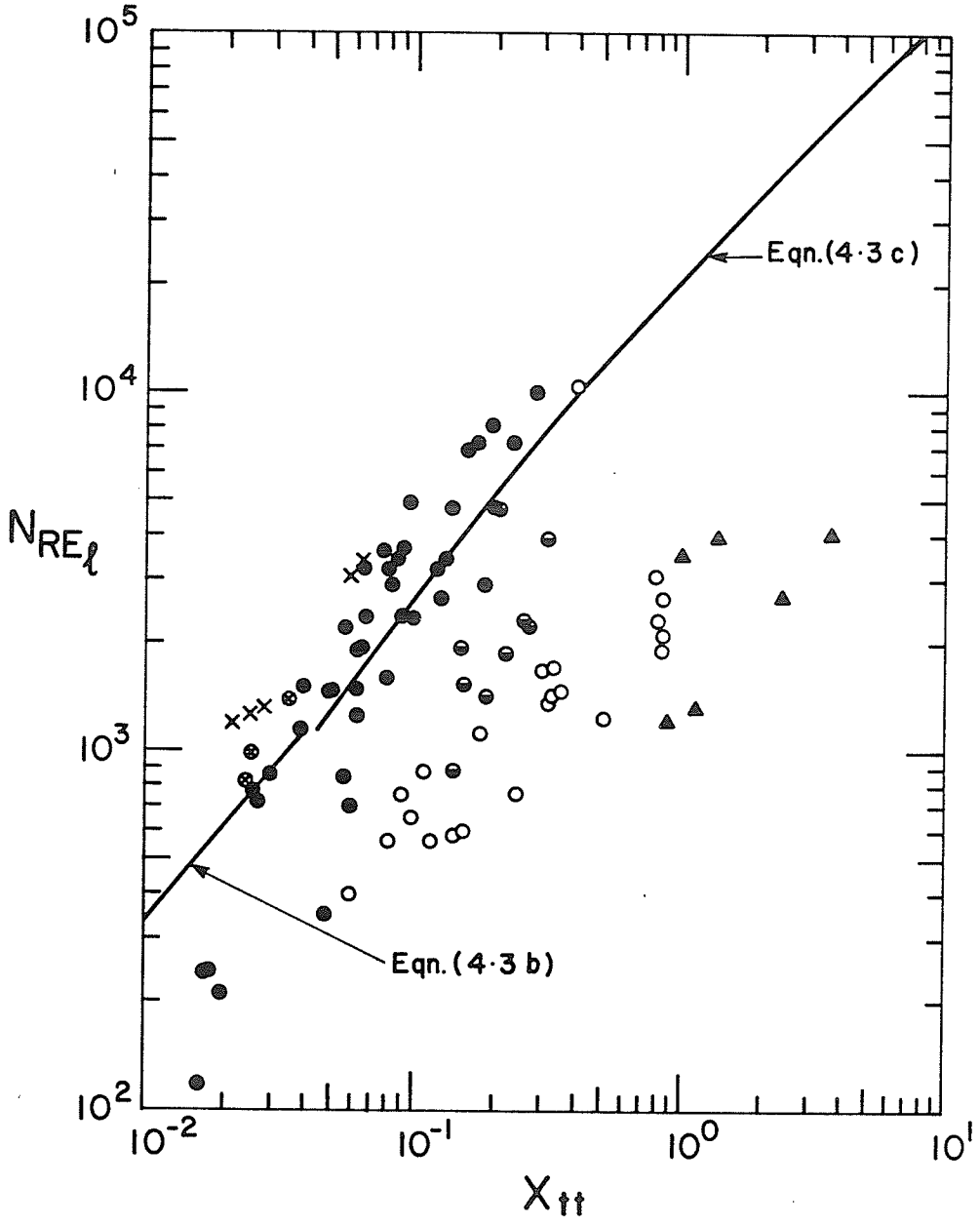

Fig. 4.10 Comparison between Soliman's [16] data of condensing Freon-12 inside a 0.5 in. horizontal tube and the theoretical prediction of Traviss and Rohsenow [18].

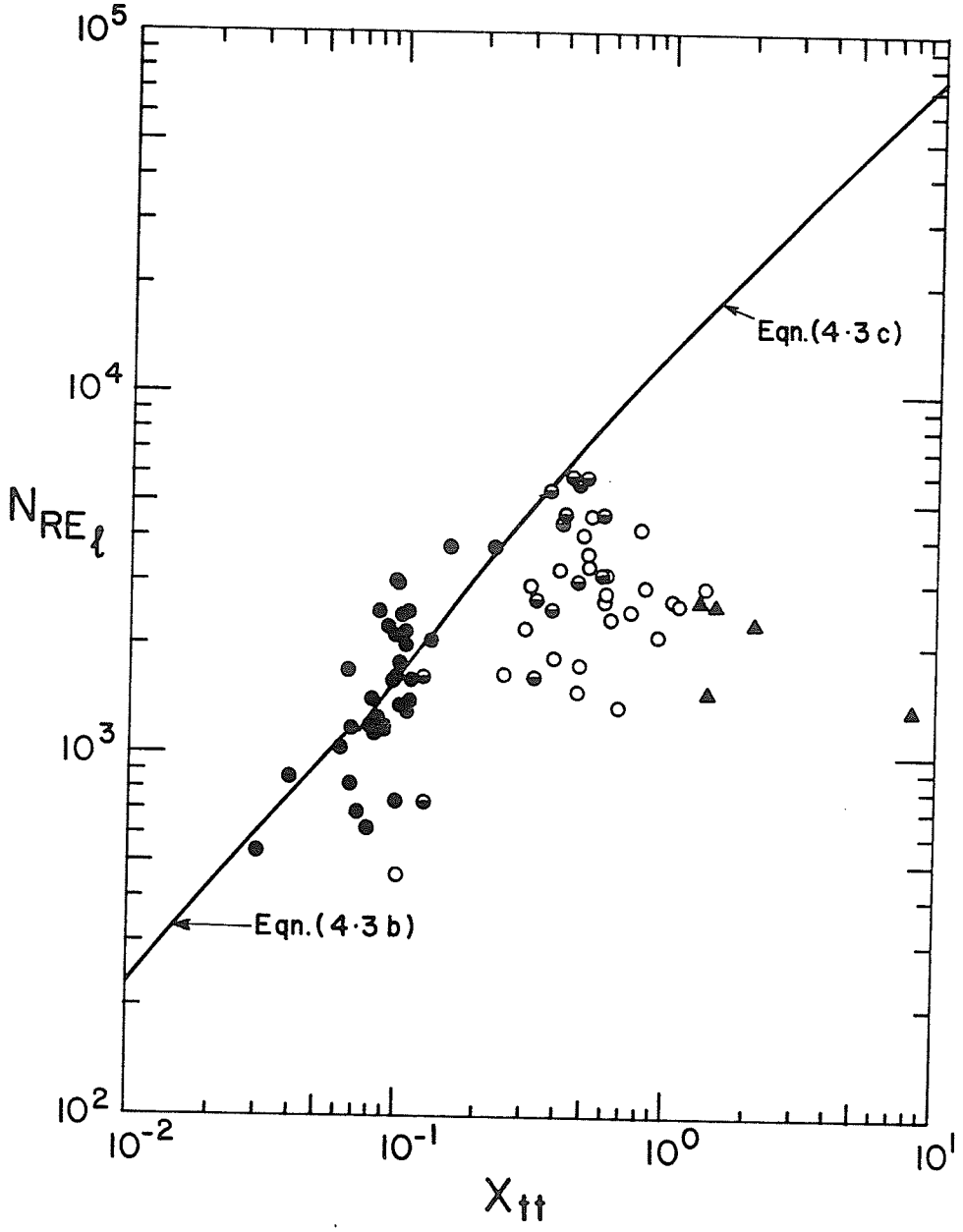

Fig. 4.11 Comparison between Soliman's [19] data of Condensing Freon-113 inside a 0.5 in. horizontal tube and the theoretical prediction of Traviss and Rohsenow [18].

using $N_{FR_\ell} = 45$ and N_{GA} evaluated at the average saturation temperature of each fluid. The boundary line still separates the annular from the wavy data points, but with a low degree of accuracy. Traviss and Rohsenow [18], after testing their criterion against data of Freon-12 [16], reported different conclusions. This discrepancy is due to the fact that Traviss and Rohsenow [18] considered the semi-annular flow reported by Soliman [16] to be in the category of stratified flow. However, according to Soliman's [16] description of this particular flow pattern it should be classified among the non-stratified flows. The lack of accuracy is due to the Froude number of the liquid ($N_{FR_\ell} = 45$), used in evaluating equations (4.3b) and (4.3c). This magnitude was determined from only the flow regime data of Freon-12 [18]. Better accuracy can be expected if it is to be determined from data of different fluids.

A more recent and more widely accepted theoretical approach is the one developed by Taitel and Dukler [14]. They used the Kelvin-Helmholtz theory for wave instability to develop dimensionless groups to correlate the transitions between different flow patterns of two-phase adiabatic flows. The two transitions which are relevant to the present study are those between annular and wavy, and annular and slug flow patterns. A summary of the analysis used by Taitel and Dukler [14] in developing these two transition lines

is provided in Appendix A. The two dimensionless groups derived by Taitel and Dukler [14], for correlating these two lines are F and X, where F is a form of Froude number, given by

$$F = \frac{G_x}{\sqrt{Dg\rho_v(\rho_\ell - \rho_v)}} , \qquad (4.4)$$

and X is a Lockhart and Martinelli [2] parameter, defined generally as

$$X = \left[\frac{(dP/dZ)_\ell}{(dP/dZ)_v}\right]^{1/2} . \qquad (4.5)$$

Coordinates of the two transition lines were calculated following the procedure suggested in [14] and the results are tabulated in Appendix A. Values of F and X for all the present observations were calculated using Equations (4.4) and (4.5) following the procedure outlined in Appendix C. A comparison between the present experimental data and these transition criteria developed by Taitel and Dukler is shown in Figure 4.12. The annular-slug transition could not be tested since the slug observations in the present study were not correlated. All spray, spray-annular, and annular observations are correctly predicted. Sixty-six percent of the wavy flow data points occupy the annular flow region. Although the accuracy of prediction is low at

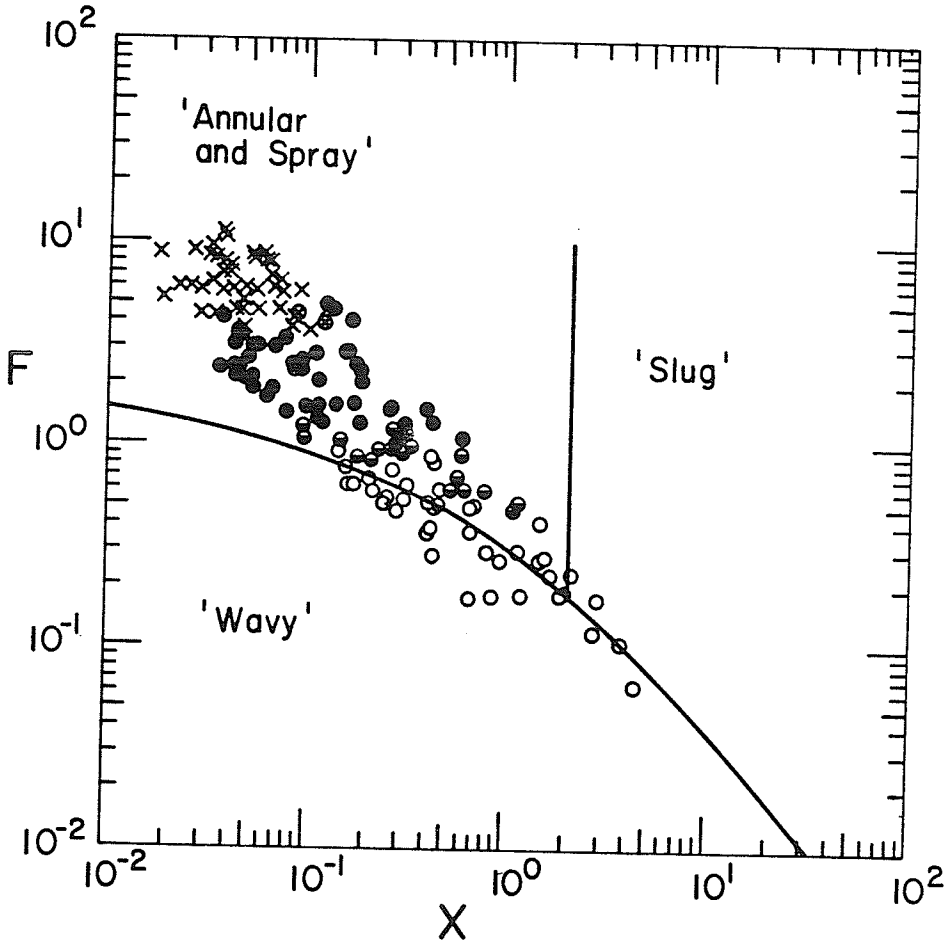

Fig. 4.12 Comparison between present data and predictions of Taitel and Dukler [14].

higher values of X (X > 0.1), the general agreement is satisfactory. This was also observed by other investigators [22] as will be discussed later. Taitel and Dukler [14] transition criteria were also tested against the data of Freon-12 [16], and Freon-113 [19] condensing inside 0.5 in. diameter tube. The results are shown in Figs. 4.13 and 4.14, respectively. Still the annular-wavy transition is fairly predicted, however, it is obvious that the annular-slug transition line failed in correlating the data. All the slug flow data points occupied the wavy region. In general, on the basis of Figs. 4.12, 4.13, and 4.14, it can be concluded that the two coordinates F and X may be used in predicting the annular and wavy flow patterns. On the other hand, there is no indication that these two parameters help in predicting the annular-slug flow transition. This last conclusion is not to be considered as a final one since it is based on a considerably small number of slug data points.

The latest effort in the attempt to define boundaries of the different flow regimes on theoretical bases is the one reported by Breber et al. [22]. Their work is based

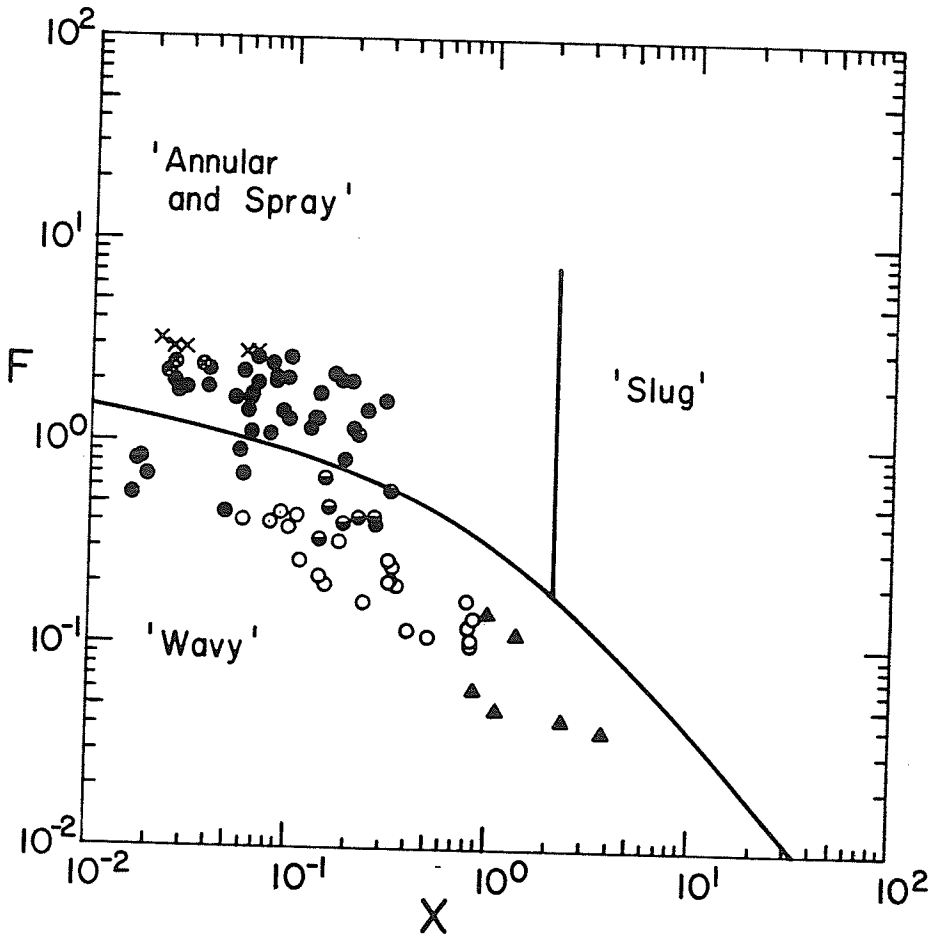

Fig. 4.13 Comparison between Soliman's [16] data of condensing Freon-12 inside a 0.5 in. horizontal tube and the predictions of Taitel and Dukler [14].

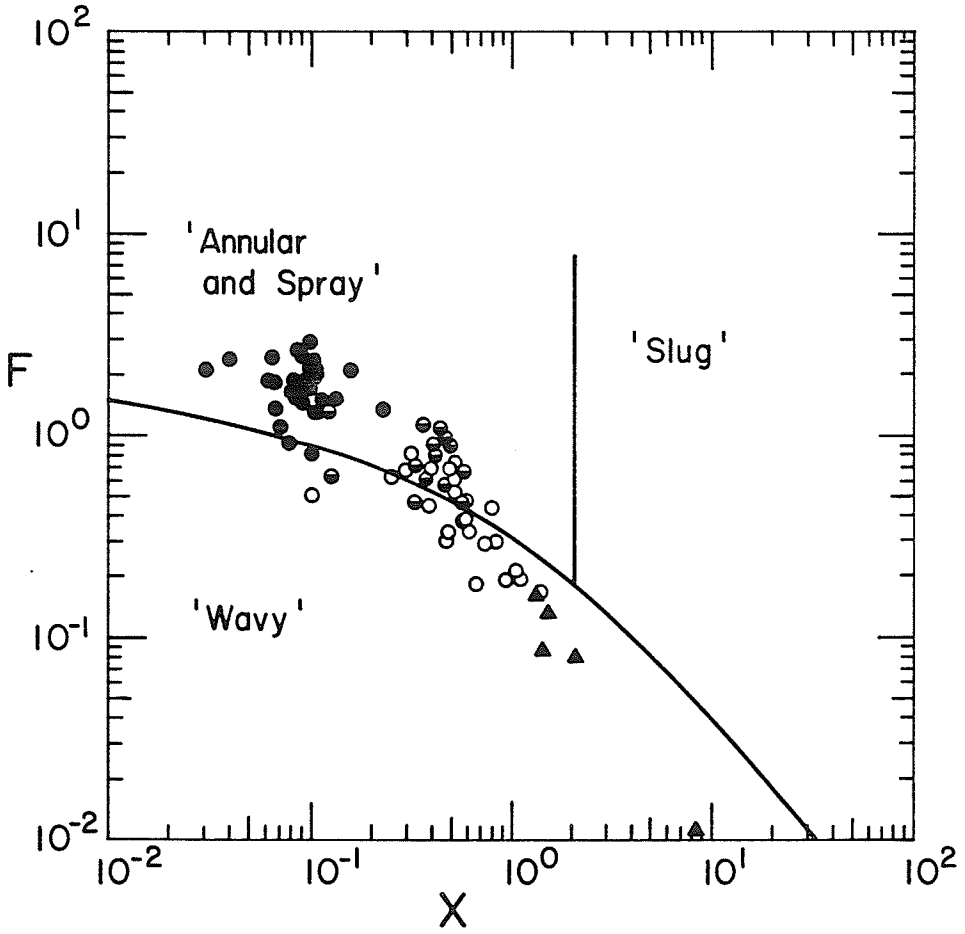

Fig. 4.14 Comparison between Soliman's [19] data of condensing Freon-113 inside a 0.5 in. horizontal tube and the predictions of Taitel and Dukler [14].

on the results reported by Taitel and Dukler [14], and they even used F and X (parameters developed in [14])as coordinates for their correlation. Breber et al. [22] proposed a map subdivided into four regions separated by transition lines and transition zones, as shown in Fig. 4.15. The transition lines of this map, although not developed from a rigorous analysis, are simple and easy to use for prediction purposes. In support of their simple, and admittedly crude criteria, Breber et al. [22] have shown a good correlation with the experimental data reported in [16], [18], [19],and other references. A comparison between the present results and this map is shown in Fig. 4.16. Although some of the wavy points occupied the slug region, agreement in general is good. In order to more specifically evaluate this map Table 4.2 was constructed. The procedure followed in constructing this table is the same used by Breber et al. [22]. The percentage of points for each flow pattern occupying a certain zone defined by the boundaries of Fig. 4.15 is calculated. With the exception of Zone III (slug and plug) the agreement for all zones is excellent. Since no slug regimes could be correlated during the present experimental investigation, the poor agreement for Zone III is to be expected. It should not take any credit out of the suitability of this map. The percentage of the total number of observations

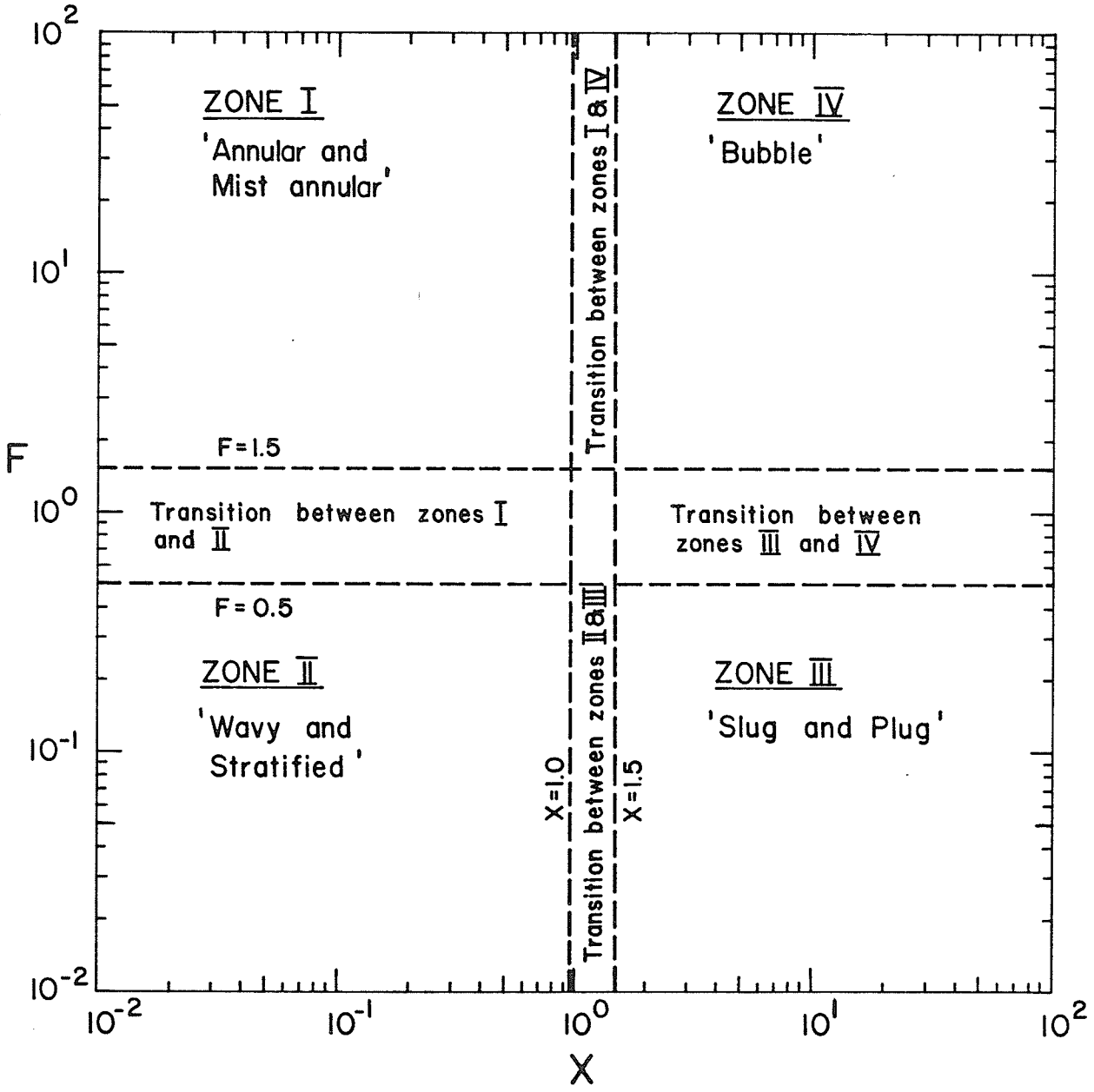

Fig. 4.15 Simplified criteria proposed by Breber et.al. [22].

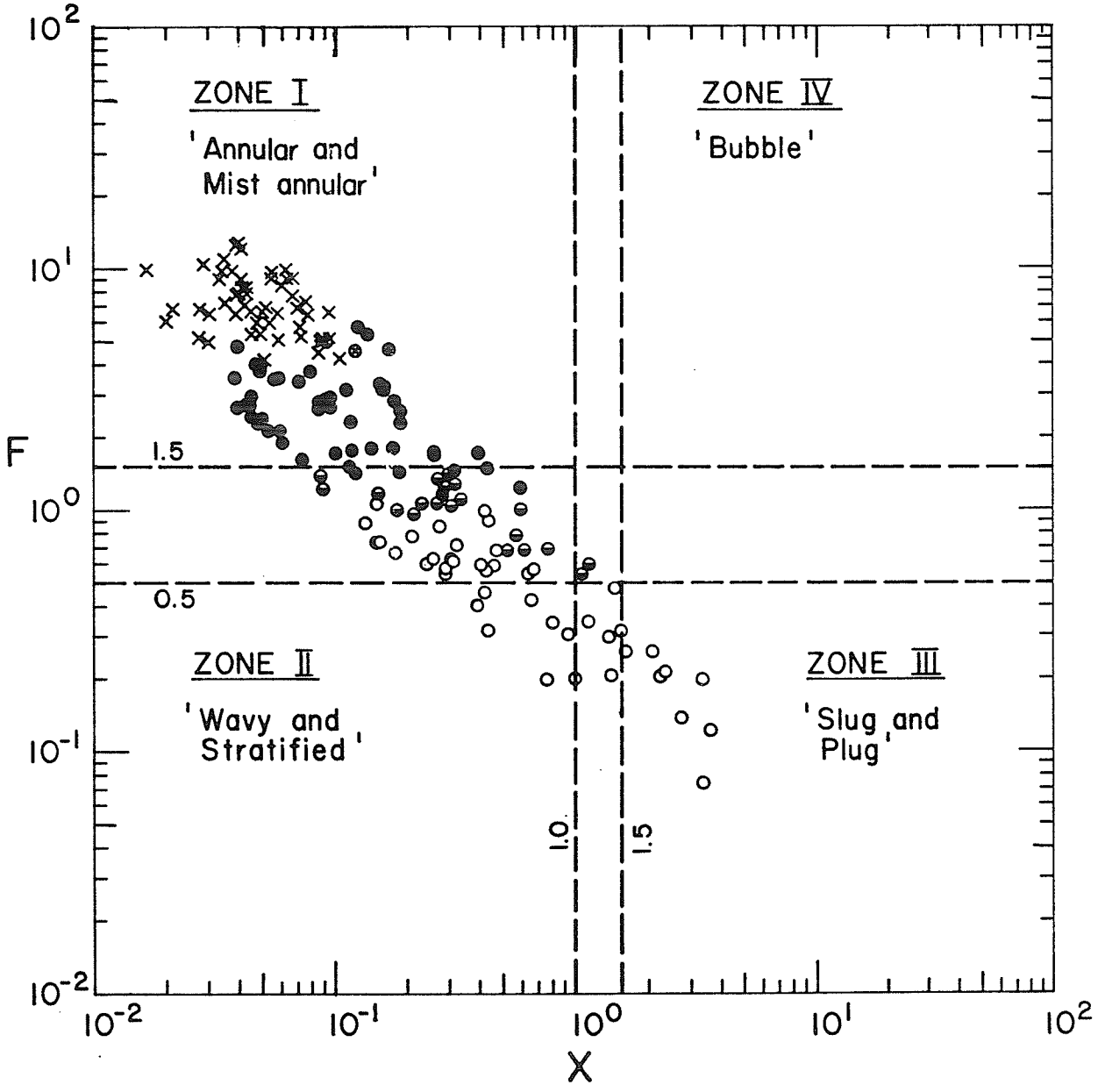

Fig. 4.16 Comparison between present data and criteria by Breber et al. [22].

Table 4.2: Distribution of the observed flow patterns.

Flow Patterns Zones	Percentage of points of each type observed in each zone			
	Annular and Mist I	Annular-Wavy Transition	Wavy and Stratified II	Slug and Plug III
Zone I Annular Mist and Annular	100	0	0	0
Zone II Wavy and Stratified	0	0	100	0
Zone III Slug and Plug	0	0	100	0
Transition Between Zones I & II	14	40	46	0
Transition Between Zones II & III	0	0	100	0

successfully predicted to occupy their respective flow regimes on the map is 96%, a value which is reflecting the overall percentage success of the Breber et al. [22] proposed correlation. Testing this correlation against the data of Freon-12 [16] and Freon-113 [19] was not found to be necessary since Breber et al. [22] have done that in their work. The results they have obtained were also good. Based on the results obtained here as well as those in [22] the two parameters X and F appears to be significant for flow patterns prediction during condensation. However the boundaries associated with these coordinates which were originally derived by Taitel and Dukler [14] need to be thoroughly tested before recommending its general use. This can be achieved by testing it against data of different fluids as well as different diameters.

4.3.3 The spray to annular transition

A common feature among all the theoretical correlations discussed in Section 4.3.2 is that the spray and annular flow patterns are included in one category. Both flow patterns are considered to be inertia controlled, and no attempt was made to study the transition criterion between them. This transition is important because it has immediate application to some practical situations, such as dry-out conditions in the cooling systems of nuclear reactors.

Soliman [16] made an initial attempt to develop an empirical correlation for the spray-annular transition. He postulated that the dominant forces influencing this transition are the inertia and surface tension forces. The spray flow would exist when the inertia forces dominate, and a stable liquid film can only exist when surface tension forces are large enough to overcome the influence of the inertia forces [16]. Based on his data of condensing Freon-12 inside a 0.5 in. horizontal tube, Soliman [16] developed this criterion for the transition,

$$\left(N_{WE}\right)_{critical} = 2,300 - 2,400 \qquad (4.6)$$

where Weber number N_{WE} was defined as

$$N_{WE} = \frac{(V_{vs} + V_{\ell s})^2 \rho_{av} D}{g_c \sigma} \qquad (4.7)$$

and the average density of the mixture ρ_{av} calculated from

$$\rho_{av} = \frac{1}{\frac{x}{\rho_v} + \frac{1 - x}{\rho_\ell}} \quad . \qquad (4.8)$$

With more data corresponding to three different tube diameters and two different fluids, Soliman [19] found that equation (4.6) failed to correlate the new data and

proposed the following criterion

$$N_{RE} = 1125\ N_{CA}^{-1.38} \tag{4.9}$$

where

$$N_{RE} = \frac{(V_{vs} + V_{\ell s})\ \rho_{av}\ D}{\mu_{\ell}} \tag{4.10}$$

and the capillary number N_{CA} is given by

$$N_{CA} = \frac{(V_{vs} + V_{s})\ \mu_{\ell}}{g_c \sigma} \quad . \tag{4.11}$$

Criterion (4.9) is shown in Fig. 4.17 along with the data of spray, annular, and spray-annular flow patterns obtained in the present investigation. Agreement is fair, thus indicating that Equation (4.9) for the spray-annular transition is reasonably independent of fluid properties over a fairly wide range.

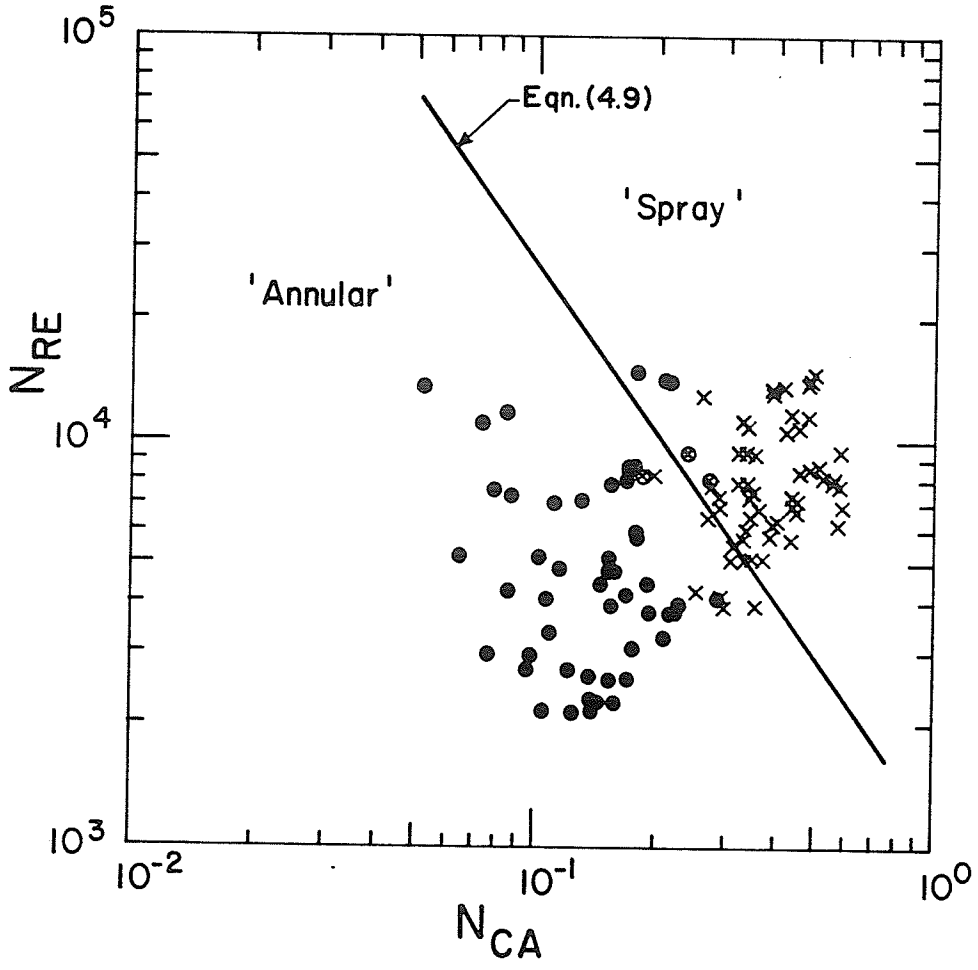

Fig. 4.17 Comparison between present data and criterion (4.9) developed by Soliman [19].

CHAPTER 5

CONCLUSIONS AND RECOMMENDATIONS

5.1 Conclusions

Before stating the specific conclusions which were drawn from the results of the present investigation, it is important to point out the following general observations regarding the two-phase flow pattern studies reported in the literature:

1. There is a fairly general agreement in the descriptions and terminology used in identifying the different flow patterns. This is important, otherwise confusion and wrong conclusions will result. Few exceptions exist where two independent investigators observed the same flow pattern, reported a similar description, but gave it two different names; (e.g., the annular-wavy flow pattern in [17] and semi-annular flow pattern in [18]). This led Traviss and Rohsenow [18] to conclude that Baker's [5] map predicted their data adequately, while Soliman and Azer [17] arrived at exactly the opposite conclusion. Recent results reported by other investigators [21], [22] supported the conclusion in [17].

2. There is no standard method for presenting the data of two-phase flow patterns. Different correlations and maps using different coordinate systems were suggested; some empirical, and others theoretical. Naturally, the lack of a standard coordinate system or systems reflects the lack of true understanding of the transition criteria between different flow patterns.
3. There is a recent trend in the literature to avoid using one coordinate system for correlating all the transition lines. Since each transition line is governed by different set of relevant parameters, hence each line should be correlated separately and no single system of coordinates is expected to provide an accurate general correlation [14].

Several conclusions were drawn from the results of the present investigation. For the sake of an orderly presentation, these conclusions will be divided into three groups; one related to the observed flow patterns, the second related to the comparisons with empirical correlations, and the third related to comparisons with theoretical predictions. Regarding the flow patterns observed in this study, the following conclusions can be made:

1. Flow patterns observed in this investigation for condensing steam inside a horizontal tube are similar

in appearance to those described in other investigations [17], [20], [21], and [22] using other test fluids, with the exception of a minor difference in the wavy flow pattern. In the present study, the upper part of the tube was always covered with a thin liquid film, while in the previously mentioned studies the upper part of the tube appeared dry during wavy flow.

2. Stratified flow existed at the outlet of the tube during test runs corresponding to low mass flow rates of stream. This flow pattern was not reported in other investigations [20], [21], and [22].

Based on the comparisons between the present results and leading empirical correlations in the literature, the following conclusions can be made:

1. Baker's [5] map failed in predicting the present results. However, when comparing the present results with a map proposed for condensation [19] using Baker's [5] coordinates a good agreement resulted. This indicates that Baker's coordinates are fairly independent of fluid properties.

2. The map proposed by Soliman [19] using V_ℓ and $(1 - \alpha)/\alpha$ as coordinates provided an adequate prediction of the present data. This supports the hypothesis [19] that V_ℓ and α are relevant parameters for flow patterns of condensing fluids and can be used

as a basis for the generation of a generalized correlation.

3. Superficial vapor and liquid velocities, used as coordinates in [12], cannot serve as a basis for the generation a generalized flow pattern correlation for condensation. Fluid properties were shown to have a strong influence on the transition lines when this coordinate system is used.

Comparisons with theoretical predictions of flow pattern transitions led to the following conclusions:

1. Good agreement was found between the present data and the criteria developed by Traviss and Rohsenow [18] using N_{RE_ℓ} and X_{tt} as coordinates. A reasonable agreement was also found with data of other fluids. However, the degree of accuracy was affected by the value of Froude number used. The value suggested by Traviss and Rohsenow [18] (N_{FR_ℓ} = 45) was based on their data for Freon-12.
2. The annular-slug boundary developed by Taitel and Dukler [14] failed in correlating the data of Freon-12 [16] and Freon-113 [19]. On the other hand, a satisfactory agreement was obtained for the annular-wavy transition line when tested against present data as well as data of Freon-12 [16] and Freon-113 [19].

This implies that the two coordinates X and F used in this correlation are significant parameters for condensation.

3. The map developed by Breber et al. [22], using Taitel and Dukler [14] coordinates agreed well with the present data. Similar results were also reported by Breber et al. [22] for Freon-12 [16] and Freon-113 [19]. This supports the significance of the parameters X and F as far as flow pattern prediction during condensation is concerned.

5.2 Recommendations for Further Studies

This investigation, similar to others reported in the literature, succeeded in answering some questions while generating new ones to be answered. The field of two-phase flow is a continuously growing field and there is an increasing interest in it because of its direct relation to many practical applications. Questions which are yet to be answered are numerous. Limiting the enquiry to the area of flow patterns of condensing fluids inside horizontal tubes, the following topics deserve immediate research efforts:

1. The influence of tube diameters on the appearance of flow patterns and on different coordinate systems used in data correlation. More data, especially for large tube diameters (I.D. $\geq$ 1 in.) are needed.

2. Data corresponding to other test fluids is still required to establish the influence of fluid properties on a more solid basis.
3. The wavy-to-slug transition needs experimental as well as theoretical analyses. Slugging in engineering devices is associated with pressure fluctuations and other damaging effects. No adequate prediction is available yet for this transition.
4. Stratification is another phenomenon which requires a special research effort. This flow pattern, observed in the present study, is sometimes undesirable in applications such as cooling systems of nuclear reactors. Conditions leading to the existence of this flow pattern are yet to be accurately defined.

REFERENCES

[1] R.C. Martinelli, L.M.K. Boelter, T.H.M. Taylor, E.G. Thomsen, and E.H. Morrin, "Isothermal Pressure Drop for Two-Phase Two-Component Flow in a Horizontal Pipe", Trans ASME, 66, 1944, pp. 139-144.

[2] R.W. Lockhart, and R.C. Martinelli, "Proposed Correlation of data for Isothermal Two-Phase Two-Component Flow in Pipes", Chem. Engg. Prog. 45, 1949, pp. 39-48.

[3] O.P. Bergelin, and C. Gazley, "Co-current Gas-Liquid Flow, 1. in. Horizontal Tubes", Proceeding of the 1949 Heat Transfer and Fluid Mechanics Institute, Berkeley, Calif., 1949, pp. 5-19.

[4] G.E. Alves, "Co-current Liquid-Gas Flow in a Pipe Contractor", Chem. Engg, Prog., 50, 1954, pp. 449-456.

[5] O. Baker, "Simultaneous Flow of Oil and Gas", Oil and Gas Journal, 53, 1954, pp. 185-195.

[6] Holmes, "Flooding Velocities in Empty Vertical Tubes", Perry's Chemical Engineers Handbook, Third Edition, McGraw-Hill Book Company, New York, 1959, Figs. 17 and 18, p. 686.

[7] C.J. Hoogendoorn, "Gas-Liquid Flow in Horizontal Pipes", Chem. Engg. Sci., 9, 1959, pp. 205-218.

[8] C.J. Hoogendoorn, and A.A. Buitelaar, "The Effect of Gas Density and Gradual Vaporization on Gas-Liquid Flow in Horizontal Pipes", Chem. Engg. Sci., 16, 1961, pp. 208-221.

[9] G.W. Govier, and M.M. Omer, "The Horizontal Pipe Line Flow of Air-Water Mixtures", Can. J. of Chem. Engg., 40, 1962, pp. 93-104.

[10] G.W. Govier, and K. Aziz, "The Flow of Complex Mixtures in Pipes", Van Nostrand-Reinhold Company, New York, 1972, pp. 516-526.

[11] D.S. Scott, "Properties of Co-current Gas-Liquid Flow, Advances in Chem. Engg., 4, 1963, pp. 209-210.

[12] J.M. Mandhane, G.A. Gregory, and K. Aziz, "A Flow Pattern Map for Gas-Liquid Flow in Horizontal Pipes", Int. J. of Multiphase Flow, 1, 1974, pp. 537-553.

[13] E. Quandt, "Analysis of Gas-Liquid Flow Patterns", Chem. Engg. Prog. Symp., Ser. 57, 61, 1965, pp. 128-135.

[14] Y. Taitel and A.E. Dukler, "A Model for Predicting Flow Regime Transitions in Horizontal and Near Horizontal Gas-Liquid Flow" AIChE J., 22, 1976, pp. 47-55.

[15] W.R. Zahn, "Flow Conditions When Evaporating Refrigerant-22 in Air-Conditioning Coils", ASHRAE Transactions, 72, Part 1, 1966, pp. 82-89.

[16] H.M. Soliman, "Visual and Photographic Flow Pattern Studied During Condensation Inside Horizontal Tubes", M.S. Thesis, Kansas State University, 1970.

[17] H.M. Soliman, and N. Azer, "Flow Patterns During Condensation Inside a Horizontal Tube", ASHRAE Trans. 77, Part 1, 1971, pp. 210-215.

[18] D.P. Traviss, and W.M. Rohsenow, "Flow Regimes in Horizontal Two-Phase Flow with Condensation", Paper Presented During the ASHRAE Spring Conference, Minneapolis, Minnesota, May 3-5, 1973, pp. 31-39.

[19] H.M. Soliman, "Analytical and Experimental Studies of Flow Patterns During Condensation Inside Horizontal Tubes", Ph.D. Dissertation, Kansas State University, 1974.

[20] H.M. Soliman, and N.Z. Azer, "Visual Studies of Flow Patterns During Condensation Inside Horizontal Tubes", Proceedings of the Fifth Int. Heat Transfer Conference, Tokyo, Japan, Vol. 1974, pp.

[21] J.W. Palen, G., Breber, and J. Taborek, "Prediction Flow Regimes in Horizontal Inside Condensation", AIChE Paper No. 5, presented at the 17th National Heat Transfer Conference, Salt Lake City, Utah, 1977, pp. 38-44.

[22] G. Breber, J.W. Palen, and J. Taborek, "Prediction of Horizontal Tubeside Condensation of Pure Components Using Flow Regime Criteria", Condensation Heat Transfer, The 18th National Heat Transfer Conference, San Diego, California, 1979, pp. 1-8.

[23] S.L. Smith, "Void Fractions in Two-Phase Flow, A Correlation Based Upon an Equal Velocity Head Model", Inst. of Mech. Engg. (London), 184, 1969-70, pp. 647-657.

[24] "Steam Tables", An ASME Publication Distributed by Combustion Engineering, Inc., Windsor, Conn., 1967.

APPENDIX A

Taitel-Dukler [14] Model for Predicting Flow Pattern Transitions in Horizontal and Near Horizontal Gas Liquid Flows

An equilibrium stratified flow as shown in Fig. A.1 is considered. The gas is flowing with a velocity U_G in the upper part of the tube. The liquid is flowing with a velocity u_L at the lower part. The interface is smooth. A momentum balance on each phase yields:

$$A_L \left(\frac{dP}{dx}\right) - \tau_{WL} S_L + \tau_i S_i + \rho_L A_L g \sin \alpha = 0 \qquad (A.1)$$

$$A_G \left(\frac{dP}{dx}\right) - \tau_{WG} S_G - \tau_i S_i + \rho_G A_G g \sin \alpha = 0 \qquad (A.2)$$

Where:

A_L = Flow cross-sectional area of the liquid.

A_G = Flow cross-sectional area of the gas.

S_L = Perimeter of the liquid.

S_G = Perimeter of the gas.

S_i = Perimeter of the interface between the liquid and the gas.

$\left(\frac{dP}{dx}\right)$ = Pressure drop.

τ_{WL} = Shear stress of liquid.

τ_{WG} = Shear stress of the gas.

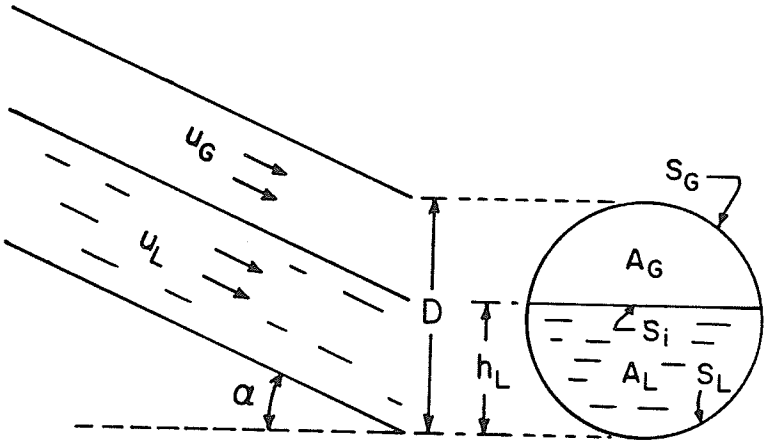

Fig. A.1. Equilibrium stratified flow.

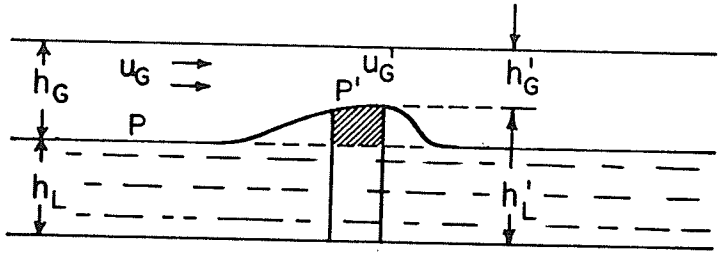

Fig. A.2. Instability for a solitary wave.

τ_{Wi} = Shear stress at the interface.

ρ_L = Density of the liquid

ρ_G = Density of the gas.

α = Angle between the pipe axis and the horizontal.

g = Acceleration of gravity.

By equating the pressure drop in the two phases, and evaluating the shear stress and the gas and liquid friction factors in the conventional

$$X^2 \left[(\tilde{U}_L \tilde{D}_L)^{-n} \tilde{U}_L^2 \frac{\tilde{S}_L}{\tilde{A}_L}\right] - \left[(\tilde{U}_G \tilde{D}_G^2)^{-m} \tilde{U}_G \left(\frac{\tilde{S}_G}{\tilde{A}_G} + \frac{\tilde{S}_i}{\tilde{A}_L} + \frac{\tilde{S}_i}{\tilde{A}_G}\right)\right] - 4Y = 0 \qquad (A.3)$$

where:

$$X^2 = \frac{\frac{4C_L}{D}(u_L^S D/\nu_L)^{-n} \cdot \frac{1}{2}(\rho_G u_L^{S2})}{\frac{4C_G}{D}(u_G^S D/\nu_G)^{-m} \cdot \frac{1}{2}(\rho_G u_G^{S2})} = \frac{\left|(dP/dx)_L\right|}{\left|(dP/dx)_G\right|}$$

(It is the same parameter introduced by Lockhart and Martinelli [2])

$$Y = \frac{(\rho_L - \rho_G)\, g \sin\alpha}{\frac{4C_G}{D}\left(\frac{u_G^S D}{\nu_G}\right)^{-m} \frac{\rho_G (u_G^S)^2}{2}} = \frac{(\rho_L - \rho_G)\, g \sin\alpha}{\left|(dP/dx)_G^S\right|}$$

m, n = Exponent of Reynold number in the equation used for evaluating the friction factor.

C_L, C_G = Friction coefficients of the liquid and the gas respectively.

ν_L, ν_G = Kinematic viscosity of the liquid and the gas respectively.

D = Diameter of the pipe.

$-u_L^s, u_G^s$ = Superficial velocity of the liquid and the gas respectively.

$-\left(\frac{dP}{dx}\right)_L^s$ = Pressure drop of the liquid phase if it is flowing alone in the pipe.

$-\left(\frac{dP}{dx}\right)_G^s$ = Pressure drop of the gas phase if it is flowing alone in the pipe.

$-\sim$ = designates dimensionless qualities.

$-$ Reference variables are D for length, D for area, superficial velocities u_L^s and u_G^s for the liquid and gas velocities respectively.

All dimensionless quantities depend only on $\tilde{h}_L = h_L/D$, since:

$$\tilde{A}_L = 0.25\ [\pi - \cos^{-1}(2\tilde{h}_L - 1) + (2\tilde{h}_L - 1)\ \sqrt{1-(2\tilde{h}_L-1)^2}]$$

$$\tilde{A}_G = 0.25\ [\cos^{-1}(2\tilde{h}_L - 1) - (2\tilde{h}_L - 1)\ \sqrt{1-(2\tilde{h}_L-1)^2}]$$

$$\tilde{S}_L = \pi - \cos^{-1}(2\tilde{h}_L - 1)$$

$$\tilde{S}_G = \cos^{-1}(2\tilde{h}_L - 1)$$

$$\tilde{S}_i = \sqrt{1-(2\tilde{h}_L - 1)^2}$$

$$\tilde{u}_L = \tilde{A}/\tilde{A}_L$$

$$\tilde{u}_G = \tilde{A}/\tilde{A}_G$$

Hence, each X-Y pair corresponds to a unique value of h_L/D for all conditions of pipe size, fluid properties, flow rate and pipe inclinations for which stratified flow exists.

Transition Between Wavy and Annular or Intermittent Patterns:

Their theoretical approach started by considering a stratified flow with a wave existing on the surface over which gas flows. This configuration is shown in Fig. A.2. The growth of the wave according to the Kelvin-Helmholtz theory will start when:

$$u_G > \left[\frac{g(\rho_L - \rho_G)h_G}{\rho_G}\right]^{1/2} .$$

This criterion is extended to the case of a finite wave on a horizontal surface. Furthermore the analysis is extended to the inclined round pipe geometry. The criterion then becomes:

$$u_G > C_2 \left[\frac{(\rho_L - \rho_G)\, g \cos \alpha\, A_G}{\rho_G\, dA_L/dA_H}\right]$$

with $C_2 \simeq A_G'/A_G$

C_2 is unity for infinitesimal disturbance where $A_G' \to A_G$. When the liquid reaches the top of the tube C_2 approaches zero. Hence C_2 was estimated, by speculation, as follows:

$$C_2 = 1 - h_L/D \ .$$

In dimensionless form, the wave growing criteria becomes:

$$F^2 \left[\frac{1}{C_2^2} \frac{\tilde{u}_G\, d\tilde{A}_L/D\tilde{h}_L}{\tilde{A}_G}\right] \geq 1 \qquad (A.6)$$

with

$$- F = \left(\frac{\rho_G}{\rho_L - \rho_G}\right)^{1/2} \frac{u_G^S}{\sqrt{Dg \cos \alpha}}$$

$$- d\tilde{A}_L/d\tilde{h}_L = (1-(2\tilde{h}_L-1)^2)^{1/2} \ .$$

Equation (A.6) describes the conditions for the transition in pipes between wavy and annular or intermittent flow patterns. All the terms in the square bracket are functions of h_L/D. Thus for any value of Y the transition can be determined from X and F. For the horizontal case (Y = 0) values of F corresponding to different values of X

are presented in Table A.1. Equation (A.6) with the equality sign was used to calculate values of F corresponding to values of h_L/D. Values of X corresponding to values of h_L/D were obtained from equation (A.3).

Transition Between Intermittent and Annular Dispersed Liquid Regimes:

It was suggested that the development of both intermittent and annular flow will depend only on the liquid level in the stratified equilibrium flow. Annular will be obtained when h_L/D is less than 0.5; while intermittent flows will exist when the equilibrium liquid level in the pipe is above the pipe centerline.

A single value of X will define this transition since it takes place at a constant value of $h_L/D = 0.5$. For horizontal tubes X = 1.6.

Table A.1: Values of F and X on the transition line between wavy and annular flow regimes.

X	F
0.024	1.251
0.040	1.118
0.070	0.976
0.135	0.808
0.221	0.680
0.332	0.575
0.473	0.484
0.653	0.406
0.884	0.337
1.186	0.275
1.584	0.222
2.123	0.174
2.874	0.134
3.963	0.099
5.621	0.070
8.330	0.047
13.217	0.028
23.499	0.015
51.823	0.006
102.996	0.003

APPENDIX B

Operating Conditions and Heat Balance

Legend:

RN	Run number
OP	Operating pressure (psia)
TSAT	Saturation temperature (°F)
G	Total mass velocity ($lb_m/hr\text{-}ft^2$) x 10^{-4}
HGW	Heat gained by the water (Btu/hr) x 10^{-4}
HLS	Heat lost by steam (Btu/hr) x 10^{-4}
ERROR	% heat balance error

OPERATING CONDITIONS & HEAT BALANCE

RN	OP	TSAT	G	HGW	HLS	ERROR
1	19.5	226.6	11.09	17.69	18.45	4.09
2	19.4	226.4	7.23	13.12	12.18	-7.74
3	17.3	220.4	4.83	7.72	8.16	5.48
4	20.5	229.4	4.07	7.09	6.90	-2.73
5	23.3	236.2	6.45	9.88	10.85	8.91
6	25.4	241.1	10.84	19.43	18.38	-5.71
7	28.9	248.3	8.51	13.30	14.27	6.80
8	19.6	226.8	8.31	13.66	13.89	1.67
9	18.2	223.0	2.74	4.85	4.63	-4.71
10	17.7	221.6	3.52	6.46	5.92	-9.11
11	19.0	225.3	5.28	8.85	8.84	-0.01
12	23.0	235.5	3.69	6.60	6.21	-6.34
13	18.3	223.2	2.88	4.91	4.85	-1.14
14	18.3	223.2	2.94	5.03	4.96	-1.41
15	18.3	223.4	4.36	7.06	7.28	3.01
16	18.1	222.7	4.65	7.63	7.70	0.93
17	18.1	222.7	5.81	9.21	9.57	3.72
18	16.6	218.4	5.48	9.38	9.13	-2.72
19	19.7	227.2	5.27	8.66	8.73	0.78
20	17.1	219.9	3.72	6.54	6.24	-4.75
21	23.6	236.9	14.66	22.34	23.71	5.80
22	23.3	236.3	14.29	23.65	23.53	-0.50
23	19.4	226.5	5.55	9.26	9.17	-0.99
24	23.7	237.1	15.57	23.35	25.17	7.26
25	23.7	237.1	15.31	25.40	24.91	-1.98
26	23.4	236.5	12.60	19.41	20.54	5.50
27	21.3	231.4	6.46	10.42	10.79	3.39
28	21.8	232.7	6.97	11.07	11.66	5.06
29	29.1	248.6	17.12	26.44	27.69	4.52
30	32.1	254.2	15.95	25.55	25.69	0.57
31	35.6	260.3	16.74	26.24	27.36	4.08
32	22.6	234.5	12.59	19.80	20.44	3.10

OPRATING CONDITIONS & HEAT BALANCE (CONT)

33	23.0	235.4	12.72	19.84	20.56	3.48
34	27.2	244.8	14.13	21.91	22.80	3.90
35	26.7	243.7	14.53	22.44	23.59	4.89
36	20.1	228.2	10.92	17.66	17.99	1.85
37	20.6	229.7	10.41	16.99	16.99	-0.01
38	20.3	228.9	10.73	17.81	17.59	-1.26
39	22.4	234.2	9.30	15.12	15.10	-0.12
40	19.7	227.2	9.63	15.53	15.82	1.78
41	19.7	227.2	8.47	13.42	13.86	3.15
42	19.7	227.2	9.12	15.19	14.93	-1.78
43	19.4	226.5	7.20	11.58	11.73	1.32
44	18.9	225.1	7.20	11.78	11.78	-0.00
45	18.2	223.1	10.41	15.78	17.00	7.17
46	17.7	221.6	9.25	15.50	15.20	-1.97
47	18.8	224.8	8.22	12.92	13.49	4.21
48	17.8	222.0	8.23	13.22	13.55	2.44
49	17.3	220.4	7.97	12.35	13.08	5.59
50	16.8	219.0	7.47	11.76	12.30	4.41
51	22.0	233.2	9.88	15.58	15.93	2.18
52	22.3	233.9	9.88	17.06	16.09	-6.08
53	22.1	233.3	10.14	16.65	16.61	-0.25
54	19.6	226.9	10.28	17.03	16.91	-0.74
55	28.8	248.1	16.74	28.31	27.22	-4.00
56	29.1	248.6	17.51	29.33	28.45	-3.08
57	16.4	217.8	3.99	6.14	6.73	8.70
58	16.4	217.8	4.10	7.24	6.93	-4.48
59	16.7	218.6	4.34	6.88	7.33	6.04
60	17.8	221.7	4.05	6.79	6.82	0.44
61	18.3	223.2	4.34	7.89	7.30	-8.17
62	22.1	233.3	6.96	10.56	11.55	8.54
63	19.6	226.9	9.90	16.03	16.47	2.65
64	18.8	224.8	9.52	15.83	16.04	1.30
65	18.8	224.8	9.65	16.16	16.25	0.58
66	18.2	223.0	3.21	5.14	5.53	6.94
67	18.2	223.0	3.23	5.13	5.58	7.94

OPRATING CONDITIONS & HEAT BALANCE (CONT)

68	18.2	223.0	3.26	5.42	5.63	3.63
69	16.0	216.3	3.18	5.26	5.48	4.00
70	16.0	216.3	3.15	5.18	5.43	4.71
71	16.0	216.3	3.18	5.25	5.48	4.16
72	16.0	216.3	3.20	5.38	5.53	2.69
73	19.3	226.2	3.61	6.15	6.17	0.35
74	19.3	226.2	3.67	6.17	6.27	1.60
75	19.3	226.2	3.78	6.37	6.46	1.45
76	19.3	226.2	4.13	6.91	7.08	2.35
77	18.6	224.1	5.59	8.34	9.27	10.06
78	18.5	224.0	5.55	9.19	9.25	0.64
79	18.3	223.4	5.92	10.14	9.88	-2.62
80	18.1	222.7	6.04	10.60	10.13	-4.65
81	19.8	227.4	6.21	10.57	10.54	-0.26
82	20.3	228.9	6.14	9.47	10.45	9.40
83	20.6	229.5	6.58	10.63	11.15	4.65
84	32.8	255.6	17.24	27.62	28.04	1.48
85	32.1	254.2	17.55	28.00	28.79	2.73
86	32.9	255.7	18.17	30.53	29.78	-2.50
87	21.1	230.8	12.89	20.24	21.14	4.26
88	20.8	230.2	11.06	17.16	18.30	6.22
89	16.5	218.1	10.18	16.58	17.18	3.52
90	19.1	225.5	11.58	17.74	19.08	7.02
91	18.3	223.4	11.32	17.53	18.66	6.03
92	18.4	223.6	11.06	18.00	18.35	1.91
93	21.3	231.4	11.60	18.76	19.26	2.60
94	21.3	231.4	11.84	19.36	19.72	1.80
95	21.3	231.4	11.84	18.93	19.57	3.31
96	18.6	224.1	8.88	14.17	14.89	4.82
97	17.6	221.3	9.14	15.20	15.52	2.09
98	24.3	238.6	7.60	11.95	12.69	5.80

APPENDIX C

Sample Calculations for Run No. 16

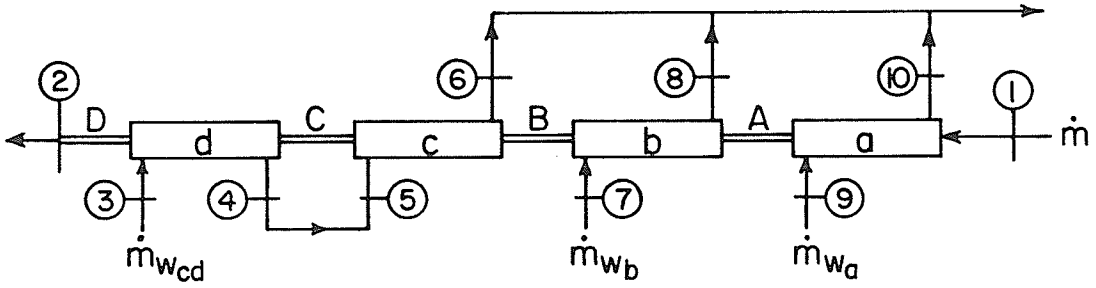

Fig. C.1 Schematic diagram of test section.

Fig. C.1 shows a schematic diagram of the test section consisting of four condensing units a,b,c, and d and four visual sections A,B,C, and D. Test fluid, with $\dot{m}$ lb_m/hr flow rate, enters as superheated vapor (state 1) and leaves as subcooled liquid (state 2). Three streams of cooling water $\dot{m}_{w_a}$, $\dot{m}_{w_b}$, and $\dot{m}_{w_{cd}}$ are used as shown. State points 3 through 10 refer to cooling water temperatures at different locations in the loop. Flow patterns at visual sections A,B, and C were observed, identified, and written

descriptions were recorded. The objective here is to show how the flow pattern parameters corresponding to each observation were calculated.

Measured Data

P_1 = 5.5 psig, P_2 = 2.5 psig, $P_{atm.}$ = 14.1 psia,

T_1 = 246.2 °F, T_2 = 104.0 °F,

T_3 = 69.4°F , T_4 = 77.4°F, T_5 = 77.6°F, T_6 = 129.8°F,

T_7 = 69.2°F , T_8 = 159.2 °F, T_9 = 69.2°F, T_{10} = 176.5°F,

$\dot{m}$ = 70.4 lb_m/hr, $\dot{m}_{w_a}$ = 339.2 lb_m/hr, $\dot{m}_{w_b}$ = 255.3 lb_m/hr , and

$\dot{m}_{w_{cd}}$ = 280.3 lb_m/hr.

Flow Patterns

At visual section A - Annular

At visual section B - Annular-wavy

At visual section C - Single-phase liquid

At visual section D - Single-phase liquid

Overall Heat Balance and Operating Conditions

Thermodynamic properties [24] of test fluid at inlet and outlet of test condenser are:

h_1 = 1165.4 Btu/lb_m and h_2 = 71.99 Btu/lb_m

Rate of heat gained by cooling water

$$\dot{Q}_w = \dot{m}_{w_a} C_p(T_{10} - T_9) + \dot{m}_{w_b} C_p(T_8 - T_7) + \dot{m}_{w_{cd}} C_p[(T_6 - T_5) + (T_4 - T_3)] = 76,300 \text{ Btu/hr}$$

Rate of heat lost by test fluid

$$\dot{Q}_s = \dot{m}\,(h_1 - h_2) = 77,000 \text{ Btu/hr}$$

$$\text{Percentage heat balance error} = \frac{77,000 - 76,300}{77,000} \times 100 = 0.93\%$$

Run was accepted since the heat balance error is within $\pm$ 10%.

$$\text{Working pressure } P = \frac{P_1 + P_2}{2} + P_{atm.} = 18.1 \text{ psia}$$

Corresponding saturation temperature $T_s = 222.7°F$

Inlet superheat $\Delta T_{sup.} = T_1 - T_{s_1} = 19.3°F$

Properties of the two-phase mixture, corresponding to P and T_s, are:

$$\rho_\ell = 59.64 \text{ lb}_m/\text{ft}^3 \quad , \quad \rho_v = 0.0453 \text{ lb}_m/\text{ft}^3$$

$$\mu_\ell = 0.655 \text{ lb}_m/\text{hr-ft} = 0.270 \text{ centipoise}$$

$$\mu_v = 0.0320 \text{ lb}_m/\text{hr-ft}$$

$$h_\ell = 190.88 \text{ Btu/lb}_m \quad , \quad h_v = 1154.8 \text{ Btu/lb}_m$$

$$\sigma = 58.8 \text{ dyne/cm}$$

$$\text{Mass velocity } G = \frac{\dot{m}}{\frac{\pi}{4} D^2} = 46,500 \text{ lb}_m/\text{hr-ft}^2$$

Qualities at Different Visual Sections

Due to inescapable experimental errors, values of $\dot{Q}_s$ and $\dot{Q}_w$ are expected to be different. Rates of heat gain by cooling water in all condensing units were adjusted by a factor J such that,

$$J = \frac{\dot{Q}_s}{\dot{Q}_w} = 1.009 \ .$$

A simple heat balance on condensing unit a produces

$$h_A = h_1 - [\dot{m}_{w_a} \cdot J \cdot C_p \cdot (T_{10} - T_9)]/\dot{m}$$

$$= 643.8 \quad Btu/lb_m$$

$$x_A = \frac{h_A - h_\ell}{h_v - h_\ell} = 0.47$$

Similarly, a heat balance on condensing units b and c resulted in

$$h_B = 314.6 \quad Btu/lb_m \ , \quad x_B = 0.128$$

$$h_C = 104.9 \quad Btu/lb_m < h_\ell \text{ (subcooled liquid at C)}$$

Flow Pattern Parameters

The steps used in calculating the flow pattern parameters at visual section A are shown here. Similar procedure was followed at visual section B.

(a) Baker's [5] Parameters

Based on equations (2.1) and (2.2)

$$\lambda = 0.760 \quad \text{and} \quad \psi = 0.827$$

$$G_v = xG = 21{,}860 \ \ lb_m/hr\text{-}ft^2$$

$$G_\ell = (1-x)G = 24{,}640 \ \ lb_m/hr\text{-}ft^2$$

$$\frac{G_v}{\lambda} = 28.740 \quad \text{and} \quad G_\ell \lambda \psi / G_v = 0.709$$

(b) Mandhane et.al. [12] Parameters

$$V_{\ell s} = \frac{(1-x)G}{\rho_\ell} = 0.115 \text{ ft/sec.}$$

$$V_{vs} = \frac{xG}{\rho_v} = 134.0 \text{ ft/sec.}$$

(c) Soliman's [19] Parameters

Using Equation (4.2), we get

$$\alpha = 0.9844$$

$$(1-\alpha)/\alpha = 0.0158$$

$$V_\ell = \frac{(1-x)G}{(1-\alpha)\rho_\ell} = 7.37 \text{ ft/sec.}$$

(d) Traviss and Rohsenow [18] Parameters

Using Equations (4.3g) and (4.3d), respectively, the following values can be obtained:

$$X_{tt} = 0.0415 \quad \text{and} \quad N_{RE_\ell} = 1653$$

(e) Taitel and Dukler [14] Parameters

The two dimensionless groups developed in [14] are F and X, defined by Equations (4.4) and (4.5), respectively. Substituting the values calculated earlier into Equation (4.4), we get

$$F = 3.106 \ .$$

The value of the parameter X depends on the type of flow in both the vapor and liquid phases (laminar or turbulent). Accordingly, four possible combinations exist. Taitel and Dukler [14] stated that the decision on whether either phase is flowing laminarly or turbulently should be based on Reynolds number evaluated from the actual velocity and the hydraulic diameter. This will definitely require a trial and error procedure. Lockhart and Martinelli [2], who were the first to develop the parameter X, suggested to base the decision on Reynolds number evaluated from the superficial velocity and the pipe diameter and then lower the critical value for laminar-turbulent transition from 2000 to 1000. Both methods, although apparently different, would lead to the same result in most cases. Values of superficial Reynolds number were calculated for the liquid and vapor phases of all present data points and were found to be consistently higher than 1000, and for a clear majority of the cases even higher than 2000. Only in one case the superficial

Reynolds number of the vapor phase was 621.4. Consequently, it was decided to assume turbulent flow in both phases, for all data points and hence for the present data point, we get

$$X = X_{tt} = 0.0415 \text{ (as calculated earlier).}$$

APPENDIX D

Flow Pattern Parameters

Legend:

X	Quality
RN	Run number
S	Visual section
XBAK	$G_\ell \lambda \psi / G_V$
YBAK	G_V / λ
VLS	$V_{\ell s}$, ft/sec
VVS	V_{vs}, ft/sec
XTT	X_{tt}
REL	N_{RE_ℓ}
F	F
XSOL	$\frac{1-\alpha}{\alpha}$
YSOL	V_ℓ , ft/sec
OBS	Observation
S	Spray
S-A	Spray-annular
A	Annular
A-W	Annular-wavy
W	Wavy

FLOW PATTERN PARAMETERS

RN	S	X	XBAK	YBAK	VLS	VVS	XTT	REL	F	XSOL	YSOL	OBS
1	A	0.344	1.23	48560.	0.340	218.3	0.069	4973.	5.250	0.0252	13.80	S
	B	0.012	51.94	1736.	0.512	7.8	1.996	7491.	0.188	0.2685	2.42	W
2	A	0.101	5.77	9269.	0.304	41.8	0.276	4439.	1.002	0.0745	4.38	A
3	A	0.222	2.17	14356.	0.175	68.4	0.113	2489.	1.552	0.0377	4.81	A
4	A	0.229	2.23	11559.	0.147	50.6	0.118	2178.	1.250	0.0399	3.83	A
5	A	0.251	2.07	18977.	0.227	78.3	0.112	3452.	2.052	0.0389	6.07	A
6	A	0.282	1.82	34468.	0.366	136.3	0.100	5694.	3.727	0.0360	10.53	S
7	A	0.050	14.40	4498.	0.382	16.7	0.654	6117.	0.486	0.1445	3.02	W
8	A	0.244	2.01	25693.	0.294	115.3	0.107	4302.	2.778	0.0367	8.30	A
9	A	0.164	3.22	5882.	0.107	27.4	0.162	1540.	0.636	0.0502	2.24	W
10	A	0.093	6.06	4360.	0.148	20.6	0.286	2126	0.471	0.0749	2.13	W
11	A	0.449	0.79	30496.	0.136	138.9	0.046	1976.	3.297	0.0174	7.93	A
	B	0.102	5.63	6937.	0.221	31.6	0.270	3220.	0.750	0.0729	3.25	W
12	A	0.119	5.13	5164.	0.153	21.4	0.253	2323.	0.558	0.0722	2.27	W
13	A	0.265	1.75	10002.	0.099	46.4	0.094	1424.	1.081	0.0326	3.13	A-W
14	A	0.154	3.46	5943.	0.116	27.6	0.173	1671.	0.642	0.0527	2.32	W

FLOW PATTERN PARAMETERS (CONT)

15	A	0.425	0.85	24241.	0.117	112.3	0.049	1688.	2.621	0.0186	6.42	A
	B	0.064	9.20	3664.	0.190	17.0	0.418	2747.	0.396	0.0975	2.14	W
16	A	0.470	0.71	28736.	0.115	134.0	0.042	1653.	3.106	0.0158	7.37	A
	B	0.128	4.27	7849.	0.189	36.6	0.209	2718.	0.849	0.0604	3.32	A-W
17	A	0.506	0.61	38701.	0.134	180.5	0.036	1923.	4.184	0.0140	9.70	A
	B	0.191	2.67	14571.	0.219	67.9	0.137	3153.	1.575	0.0440	5.19	A
18	A	0.384	0.98	28709.	0.157	139.4	0.055	2213.	3.103	0.0204	7.86	A
	B	0.061	9.44	4531.	0.239	22.0	0.423	3373.	0.490	0.0963	2.72	W
19	A	0.420	0.90	27977.	0.143	125.1	0.052	2094.	3.025	0.0196	7.43	A
	B	0.088	6.72	5873.	0.224	26.3	0.317	3292.	0.635	0.0822	2.95	W
20	A	0.446	0.77	22375.	0.096	107.1	0.044	1364.	2.419	0.0167	5.83	A
	B	0.066	8.64	3337.	0.162	16.0	0.392	2298.	0.361	0.0921	1.92	W
21	A	0.442	0.88	75481.	0.384	309.4	0.052	5880.	8.161	0.0199	19.72	S
	B	0.071	9.15	12097.	0.640	49.6	0.426	9787.	1.308	0.1042	6.78	A
22	A	0.417	0.97	69804.	0.391	287.6	0.057	5969.	7.547	0.0215	18.59	S
	B	0.026	25.74	4395.	0.653	18.1	1.080	9970.	0.475	0.1900	4.09	A-W
23	A	0.466	0.74	32905.	0.139	148.1	0.044	2027.	3.557	0.0167	8.46	A
	B	0.122	4.65	8625.	0.228	38.8	0.227	3330.	0.932	0.0650	3.73	A-W
24	A	0.399	1.05	72204.	0.440	295.4	0.061	6732.	7.807	0.0230	19.51	S
	B	0.077	8.34	13980.	0.675	57.2	0.393	10331.	1.512	0.0986	7.52	A

FLOW PATTERN PARAMETERS (CONT)

25	A	0.448	0.86	79710.	0.397	326.1	0.051	6081.	8.618	0.0195	20.74	S
	B	0.009	76.62	1608.	0.712	6.6	2.887	10910.	0.174	0.3585	2.70	W
26	A	0.379	1.14	55762.	0.367	229.3	0.065	5611.	6.029	0.0245	15.33	S
	B	0.007	103.23	985.	0.587	4.0	3.772	8972.	0.106	0.4264	1.96	W
27	A	0.110	5.44	8651.	0.269	37.2	0.264	4025.	0.935	0.0736	3.93	A-W
28	A	0.029	22.27	2480.	0.317	10.5	0.942	4761.	0.268	0.1715	2.16	W
29	A	0.414	1.07	75116.	0.473	278.5	0.063	7598.	8.122	0.0242	20.04	S
	B	0.055	12.90	10037.	0.763	37.2	0.593	12250.	1.085	0.1356	6.39	A
30	A	0.333	1.57	53791.	0.504	190.2	0.090	8265.	5.817	0.0336	15.48	S
31	A	0.271	2.20	43877.	0.579	147.6	0.123	9734.	4.745	0.0444	13.63	S
32	A	0.378	1.13	56582.	0.367	236.8	0.064	5562.	6.117	0.0242	15.57	S
	B	0.037	17.86	5532.	0.569	23.2	0.775	8613.	0.598	0.1525	4.30	A-W
33	A	0.350	1.28	52440.	0.388	217.7	0.073	5902.	5.670	0.0269	14.83	S
	B	0.017	39.22	2593.	0.586	10.8	1.576	8916.	0.280	0.2407	3.02	W
34	A	0.406	1.08	62751.	0.395	240.4	0.063	6247.	6.785	0.0240	16.84	S
	B	0.053	13.09	8218.	0.630	31.5	0.597	9964.	0.889	0.1342	5.33	A-W
35	A	0.372	1.23	59520.	0.430	230.0	0.071	6766.	6.435	0.0268	16.47	S
	B	0.013	54.55	2117.	0.675	8.2	2.151	10628.	0.229	0.3054	2.89	W
36	A	0.347	1.23	47571.	0.333	219.7	0.069	4911.	5.143	0.0253	13.48	S
	B	0.015	42.09	2098.	0.503	9.3	1.657	7409.	0.227	0.2404	2.59	W

FLOW PATTERN PARAMETERS (CONT)

37	A	0.414	0.94	53411.	0.285	233.5	0.054	4232.	5.774	0.0204	14.26	S
	B	0.092	6.55	11835.	0.442	51.7	0.311	6561.	1.279	0.0819	5.84	A
38	A	0.306	1.49	40976.	0.348	180.4	0.082	5145.	4.430	0.0295	12.14	S
	B	0.018	35.29	2449.	0.493	10.8	1.416	7281.	0.265	0.2183	2.75	W
39	A	0.515	0.64	57086.	0.212	239.7	0.039	3199.	6.172	0.0151	14.22	S
	B	0.094	6.56	10460.	0.395	43.9	0.315	5972.	1.131	0.0839	5.10	A-W
40	A	0.345	1.24	41975.	0.295	187.7	0.069	4325.	4.538	0.0253	11.93	S
	B	0.023	27.84	2779.	0.440	12.4	1.140	6448.	0.300	0.1887	2.77	W
41	A	0.457	0.77	49049.	0.215	219.4	0.045	3151.	5.303	0.0172	12.68	S
	B	0.084	7.08	9019.	0.363	40.3	0.332	5319.	0.975	0.0848	4.64	A-W
42	A	0.433	0.85	49985.	0.241	223.6	0.049	3541.	5.404	0.0187	13.15	S
	B	0.064	9.53	7363.	0.399	32.9	0.434	5850.	0.796	0.1016	4.33	W
43	A	0.584	0.46	53604.	0.140	241.3	0.028	2045.	5.795	0.0110	12.88	S
	B	0.160	3.40	14663.	0.283	66.0	0.171	4136.	1.585	0.0528	5.63	A
44	A	0.472	0.71	43827.	0.177	199.8	0.042	2579.	4.738	0.0161	11.22	S
	B	0.091	6.42	8417.	0.306	38.4	0.303	4445.	0.910	0.0790	4.17	A-W
45	A	0.290	1.54	39605.	0.344	184.1	0.084	4963.	4.281	0.0296	11.97	S
	B	0.047	12.85	6380.	0.462	29.7	0.564	6666.	0.690	0.1183	4.37	A-W
46	A	0.293	1.50	36020.	0.304	169.7	0.081	4360.	3.894	0.0289	10.85	S
	B	0.005	127.22	599.	0.428	2.8	4.426	6139.	0.065	0.4391	1.40	W

FLOW PATTERN PARAMETERS (CONT)

47	A	0.511	0.61	54233.	0.188	247.9	0.037	2727.	5.863	0.0140	13.56	S
	B	0.103	5.55	10962.	0.344	50.1	0.266	4998.	1.185	0.0721	5.12	A-W
48	A	0.539	0.54	58663.	0.177	275.4	0.032	2534.	6.342	0.0124	14.44	S
	B	0.051	11.74	5504.	0.364	25.8	0.519	5217.	0.595	0.1116	3.62	W
49	A	0.386	0.98	41314.	0.228	196.9	0.055	3242.	4.466	0.0206	11.29	S
	B	0.094	5.96	10045.	0.336	47.9	0.281	4786.	1.086	0.0737	4.89	A-W
50	A	0.430	0.81	43659.	0.198	210.8	0.046	2797.	4.720	0.0175	11.51	S
	B	0.055	10.51	5577.	0.328	26.9	0.467	4641.	0.603	0.1029	3.51	W
51	A	0.455	0.81	54070.	0.252	229.0	0.048	3801.	5.846	0.0184	14.00	S
	B	0.114	5.25	13602.	0.410	57.6	0.257	6177.	1.471	0.0725	6.07	A
52	A	0.457	0.81	53929.	0.252	226.9	0.048	3801.	5.830	0.0184	13.94	S
	B	0.047	13.83	5551.	0.442	23.4	0.615	6669.	0.600	0.1311	3.81	A-W
53	A	0.457	0.81	55673.	0.258	235.5	0 048	3890.	6.019	0.0183	14.40	S
	B	0.014	48.79	1674.	0.469	7 1	1.910	7066.	0.181	0.2697	2.21	W
54	A	0.487	0.68	63536.	0.246	284.9	0.040	3610.	6.869	0.0155	16.11	S
	B	0.009	75.16	1116.	0.476	5.0	2.785	6979.	0.121	0.3330	1.91	W
55	A	0.423	1.03	75354.	0.456	280.5	0.061	7299.	8.148	0.0234	19.96	S
	B	0.027	27.14	4808.	0.769	17.9	1.157	12312.	0.520	0.2088	4.45	A-W
56	A	0.434	0.98	80585.	0.468	298.8	0.059	7508.	8.714	0.0226	21.17	S
	B	0.021	35.65	3853.	0.810	14.3	1.479	12994.	0.417	0.2452	4.11	W

FLOW PATTERN PARAMETERS (CONT)

57	A	0.223	2.11	12207.	0.144	59.6	0.110	2026.	1.320	0.0366	4.08	A
58	A	0.144	3.61	8106.	0.163	39.6	0.178	2297.	0.876	0.0528	3.25	A-W
59	A	0.084	6.61	4992.	0.185	24.2	0.307	2606.	0.540	0.0778	2.56	W
60	A	0.178	2.88	9570.	0.155	45.1	0.146	2218.	1.035	0.0462	3.51	A-W
61	A	0.090	6.38	5111.	0.184	23.7	0.300	2651.	0.552	0.0780	2.54	W
62	E	0.662	0.35	55346.	0.110	234.1	0.022	1661.	5.984	0.0087	12.84	S
	A	0.288	1.68	24039.	0.232	101.7	0.092	3502.	2.599	0.0329	7.29	A
63	E	0.520	0.60	65299.	0.222	292.8	0.036	3254.	7.059	0.0139	16.23	S
	A	0.149	3.71	18703.	0.394	83.9	0.186	5769.	2.022	0.0561	7.41	A
64	E	0.512	0.61	62934.	0.217	287.7	0.036	3149.	6.804	0.0140	15.72	S
	A	0.094	6.18	11514.	0.403	52.6	0.293	5848.	1.245	0.0771	5.62	A-W
65	E	0.496	0.65	61778.	0.227	282.4	0.039	3300.	6.679	0.0148	15.58	S
	A	0.065	9.20	8090.	0.421	37.0	0.419	6118.	0.875	0.0982	4.71	W
66	E	0.516	0.59	21698.	0.072	100.9	0.035	1042.	2.346	0.0135	5.41	A
	A	0.171	3.06	7172.	0.124	33.4	0.155	1785.	0.775	0.0485	2.68	W
67	E	0.465	0.72	19746.	0.081	91.8	0.042	1161.	2.135	0.0161	5.08	A
	A	0.127	4.34	5381.	0.132	25.0	0.212	1896.	0.582	0.0611	2.29	W
68	E	0.438	0.81	18753.	0.085	87.2	0.047	1231.	2.027	0.0177	4.92	A
	A	0.113	4.92	4858.	0.135	22.6	0.238	1943.	0.525	0.0662	2.17	W
69	E	0.393	0.93	17377.	0.089	86.0	0.052	1250.	1.878	0.0193	4.72	A

FLOW PATTERN PARAMETERS (CONT)

	A	0.059	9.61	2596.	0.139	12.9	0.428	1938.	0.281	0.0962	1.58	W
70	E	0.353	1.10	15483.	0.094	76.7	0.061	1319.	1.674	0.0221	4.36	A
	A	0.037	15.66	1614.	0.141	8.0	0.665	1965.	0.175	0.1277	1.24	W
71	E	0.297	1.42	13143.	0.104	65.1	0.076	1447.	1.421	0.0270	3.94	A
72	E	0.253	1.77	11276.	0.111	55.8	0.094	1553.	1.219	0.0320	3.59	A-W
73	E	0.479	0.70	22056.	0.088	99.5	0.041	1282.	2.384	0.0159	5.62	A
	A	0.187	2.81	8599.	0.137	38.8	0.144	2001.	0.930	0.0463	3.09	W
74	E	0.419	0.89	19593.	0.099	88.4	0 052	1453.	2.118	0.0195	5.21	A
	A	0.135	4.14	6304.	0.148	28.4	0.205	2164.	0.682	0.0602	2.61	W
75	E	0.360	1.15	17350.	0.113	78.3	0.065	1653.	1.876	0.0238	4.86	A
	A	0.097	6.01	4679.	0.159	21.1	0.286	2330.	0.506	0.0763	2.25	W
76	E	0.267	1.78	14048.	0.141	63.4	0.096	2067.	1.519	0.0333	4.38	A
	A	0.031	20.17	1634.	0.187	7.4	0.851	2731.	0.177	0.1562	1.38	W
77	E	0.688	0.29	49947.	0.081	229.8	0.018	1175.	5.400	0.0071	11.48	S
	A	0.443	0.80	32142.	0.145	147.9	0.046	2101.	3.475	0.0176	8.40	A
	B	0.067	8.86	4856.	0.243	22.3	0.404	3520.	0.525	0.0956	2.78	W
78	E	0.577	0.47	41665.	0.109	192.0	0.029	1585.	4.504	0.0110	10.05	S
	A	0.297	1.50	21474.	0.182	98.9	0.082	2632.	2.321	0.0291	6.43	A
79	E	0.527	0.57	40770.	0.130	188.8	0.034	1882.	4.407	0.0131	10.09	S
	A	0.299	1.48	23090.	0.193	106.9	0.081	2792.	2.496	0.0288	6.91	A

FLOW PATTERN PARAMETERS (CONT)

80	E	0.434	0.82	34493.	0.159	160.8	0.047	2292.	3.729	0.0179	9.07	S
	A	0.147	3.65	11674.	0.240	54.4	0.181	3455.	1.262	0.0545	4.65	A
81	E	0.354	1.19	27760.	0.188	123.9	0.067	2755.	3.001	0.0246	7.81	A
	A	0.061	10.10	4751.	0.273	21.2	0.458	4006.	0.514	0.1052	2.86	W
82	E	0.282	1.68	21554.	0.206	94.9	0.091	3049.	2.330	0.0323	6.59	A
	A	0.022	29.39	1677.	0.281	7.4	1.201	4151.	0.181	0.1966	1.71	W
83	E	0.279	1.71	22788.	0.222	99.7	0.093	3290.	2.464	0.0328	6.99	A
	A	0.034	18.78	2776.	0.298	12.1	0.803	4409.	0.300	0.1528	2.24	W
84	E	0.581	0.57	100557.	0.342	351.6	0.036	5640.	10.874	0.0144	24.13	S
	A	0.267	2.17	46263.	0.598	161.8	0.121	9870.	5.003	0.0432	14.44	A
85	E	0.564	0.61	100275.	0.363	354.6	0.038	5951.	10.843	0.0152	24.28	S
	A	0.244	2.43	43466.	0.628	153.7	0.133	10305.	4.700	0.0468	14.06	A
86	E	0.576	0.58	104826.	0.365	366.3	0.037	6030.	11.336	0.0147	25.23	S
	A	0.206	3.05	37600.	0.683	131.4	0.164	11273.	4.066	0.0554	13.02	A
87	E	0.560	0.53	88484.	0.266	382.7	0.032	3961.	9.566	0.0125	21.51	S
	A	0.232	2.21	36661.	0.464	158.6	0.117	6909.	3.964	0.0399	12.08	S-A
88	E	0.615	0.42	83842.	0.199	364.8	0.026	2964.	9.064	0.0101	19.85	S
	A	0.300	1.55	40949.	0.362	178.2	0.085	5384.	4.427	0.0305	12.22	S-A
89	E	0.541	0.52	75384.	0.217	367.1	0.031	3062.	8.149	0.0119	18.53	S
	A	0.101	5.39	14113.	0.425	68.7	0.256	5990.	1.526	0.0685	6.63	A

FLOW PATTERN PARAMETERS (CONT)

90	E	0.502	0.64	74657.	0.269	339.0	0.038	3917.	8.071	0.0145	18.75	S
	A	0.177	3.00	26230.	0.445	119.1	0.153	6483.	2.836	0.0483	9.66	S-A
91	E	0.525	0.57	77670.	0.250	359.7	0.034	3617.	8.397	0.0132	19.25	S
	A	0.155	3.45	22875.	0.446	105.9	0.173	6438.	2.473	0.0527	8.91	A
92	E	0.551	0.52	79584.	0.231	368.1	0.031	3342.	8.603	0.0120	19.45	S
	A	0.146	3.70	21068.	0.440	97.4	0.184	6361.	2.278	0.0552	8.41	A
93	E	0.500	0.67	70756.	0.272	304.3	0.040	4059.	7.650	0.0155	17.79	S
	A	0.183	2.99	25915.	0.444	111.5	0.154	6632.	2.802	0.0495	9.40	A
94	E	0.544	0.56	78595.	0.253	338.0	0.034	3777.	8.497	0.0133	19.27	S
	A	0.179	3.07	25902.	0.455	111.4	0.158	6801.	2.800	0.0504	9.48	A
95	E	0.518	0.62	74841.	0.267	321.9	0.038	3995.	8.091	0.0146	18.62	S
	A	0.187	2.92	26944.	0.451	115.9	0.151	6743.	2.913	0.0488	9.70	A
96	E	0.696	0.28	80294.	0.126	369.4	0.018	1823.	8.680	0.0069	18.40	S
	A	0.473	0.71	54546.	0.218	251.0	0.042	3161.	5.897	0.0159	13.96	S
97	E	0.440	0.79	53578.	0.238	253.3	0.046	3409.	5.792	0.0173	14.03	S
	A	0.038	15.74	4629.	0.409	21.9	0.674	5855.	0.500	0.1317	3.52	W
98	E	0.638	0.40	55762.	0.129	225.2	0.026	1991.	6.029	0.0100	13.05	S
	A	0.349	1.32	30490.	0.233	123.2	0.075	3584.	3.297	0.0277	8.63	A